6. RESEARCH PROGRAM, ACCOMPLISHMENTS, AND PLANS

Period: March 16, 2005 to March 15, 2006

RESEARCH PROGRAM

Our Nanoscale Science and Engineering Center develops tools to study nanoscale systems. We would like to control electrons and photons in nanostructures to develop future electronic and photonic devices. The Center plans to do this by synthesizing nanoscale building blocks and developing new imaging techniques. We would also like to understand better how biological systems function at the nanoscale by developing tools based on the Physical Sciences.

Three Research Clusters address these goals:

Cluster I: Tools for Integrated Nanobiology builds bridges between the Physical Sciences, Biology, and Medicine. The Physical Sciences offer powerful new tools for manipulating and testing biological cells and tissues, based on microfluidic systems, soft lithography, and semiconductor technology. In turn, Biology and Medicine offer an enormous range of engaging problems in functional biological systems, and the opportunity to think about "hybrid" systems that combine biological and non-biological components.

Cluster II: Nanoscale Building Blocks addresses the synthesis of new classes of nanostructures that exhibit size-dependent properties. An emphasis is placed on structures with unconventional shapes, as well as on zero, one and two-dimensional nanostructures including nanoparticles and nanowires. Techniques to synthesize nanostructures from new materials are being developed, including oxide semiconductors and metal chalcogenides. These nanoscale building blocks provide new approaches for ultrasmall electronics and photonics as well as sensors for biological systems.

Cluster III: Imaging at the Nanoscale explores new ways to image the quantum behavior of electrons and photons in nanostructures using custom-made scanning probe microscopes (SPMs). New instruments include a liquid-He cooled Scanning Tunneling Microscope (STM) and a Nearfield Scanning Optical Microscope with custom tips. These add to previously developed instruments for Ballistic Electron Emission Microscopy (BEEM), a dual tipped STM, and cooled SPMs for capacitive probing of electrons. These tools are used to develop ultrasmall devices for electronics and photonics, and to control single electrons for quantum information processing. Semiconductor heterostructures with novel properties are grown for this work using Molecular Beam Epitaxy (MBE) at UC Santa Barbara.

CLUSTER 1: Tools for Integrated Nanobiology

***Coordinator*: George M. Whitesides**

Donhee Ham (DEAS, Harvard)	Howard A. Stone (DEAS, Harvard)
Eric Mazur (DEAS, Physics, Harvard)	George M. Whitesides (Chemistry, Harvard)
Joseph Mizgerd (SPH, Harvard)	Xiaowei Zhuang (Chemistry, Physics, Harvard)
Kevin (Kit) Parker (DEAS, Harvard)	

***Collaborators*:** Rick Rogers (School of Public Health, Harvard), Giannoula Klement (Children's Hospital, Harvard), Ralph Weissleder (Medical School, Harvard), Mara Prentiss (Physics, Harvard), and X. Sunney Xie (Chemistry, Harvard)

Number of postdoctoral fellows: 2
Number of graduate students: 6
Number of undergraduate students: 4

Introduction

As biology begins to ask more quantitative and analytical questions about the nature of the cell, it needs new tools to study subcellular structures that have nanoscale dimensions. An important task is to build bridges between the physical and biological sciences. The physical sciences offer to biology new measurement tools and new procedures for analyzing the information obtained. In turn, biology offers to the physical sciences an enormous range of engaging problems, and stimulating examples of very sophisticated, functional biological systems. It also offers the opportunity to think about "hybrid" systems that combine biological and non-biological components.

The interface between the biological and physical sciences is one with enormous promise for fundamentally new science, and, ultimately, technology. By supporting collaborations between investigators in the Division of Engineering and Applied Sciences (DEAS), the Dept of Chemistry and Chemical Biology, the Medical School, and the School of Public Health at Harvard, Cluster I will catalyze and expand a series of very effective collaborations across the physical-biological interface.

We expect three outcomes:

Tools for Cellular Biology and Tissue Culture: One of the major contributions that the physical sciences can offer to biology are new physical tools that can provide new kinds of information about cells and tissues.

The Science and Engineering of Interfaces between Animate and Inanimate Systems: This research will contribute to studies of cells in cell cultures, and to the assembly of groups of cells of the same or different types. In society, it will contribute to engineering the interface between patients and prostheses.

Tools for the Development of Drugs: The control over cells afforded by new microfluidic tools will be the basis for entirely new types of bioassay that will be important as the pharmaceutical industry moves away from information-poor animal

assays in preclinical studies toward more informative studies based on primary human cells.

Major Accomplishments

This is a new Cluster, added to the Center for its renewal. The Center is extending our connections with the Medical community, through a new collaboration with Ralph Weissleder at Harvard's Medical School and Massachusetts General Hospital. We are building up connections with the new MIT-Harvard NanoMedical Consortium, a Center for Cancer Nanotechnology Excellence (CCNE) funded last fall by the National Cancer Institute; Ralph Weissleder and Robert Langer of MIT are co-PIs.

Microcoil Array-Based RF Cell Sensors in the CMOS/Microfluidic Hybrid System

Donhee Ham
Electrical Engineering, Harvard University
***Collaborator*:** Robert M. Westervelt (Harvard), Ralph Weissleder (Harvard Medical School)

Proposed Goal: In our previous work, we developed a CMOS/Microfluidic hybrid system combining a CMOS integrated circuit (IC) with a microfluidic system fabricated on top (Lee *et al.*, 1005, 2006; Liu *et al.*, 2005). This hybrid system, illustrated in Figure 6.1, was developed for manipulation of individual biological cells. The CMOS chip produces spatially patterned microscopic magnetic fields using an array of microcoils. By dynamically reconfiguring the magnetic field pattern, the CMOS chip can manipulate individual biological cells attached to magnetic beads that are suspended inside the microfluidic system. The microcoil is operated by integrated digital electronics that facilitate low-power operation and miniaturization of the overall system. Figure 6.2(a) shows the die micrograph of our first CMOS prototype, which was put together with a microfluidic system [Figure 6.2(b)] to successfully demonstrate manipulation of individual bead-bound biological cells: It was able to simultaneously manipulate more than 20 individual bead-bound cells with a *dc* power consumption of only 27 mW.

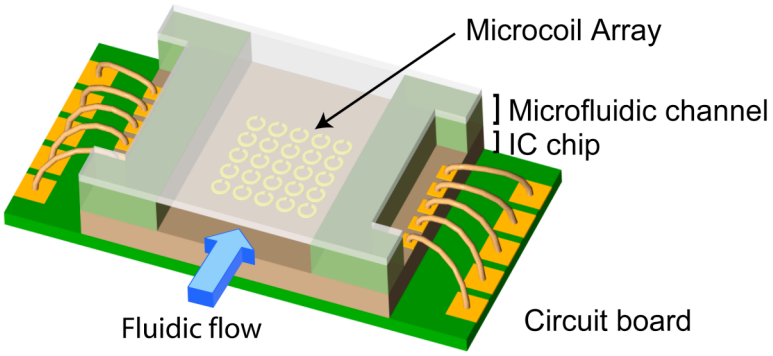

Figure 6.1. Conceptual illustration of a CMOS/Microfluidic hybrid microsystem.

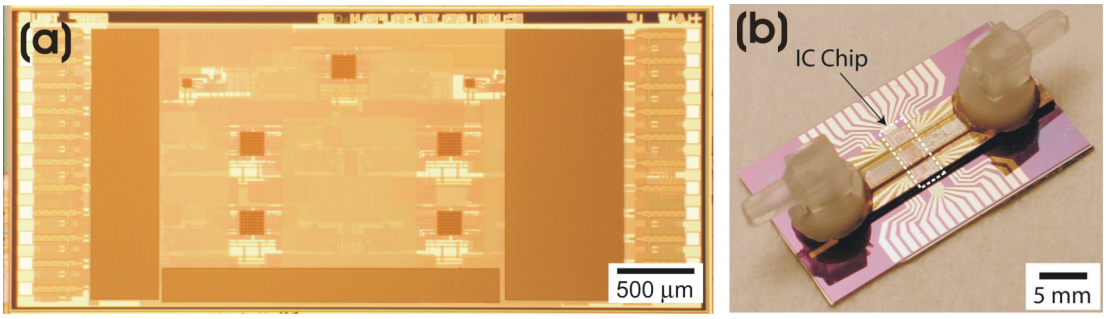

Figure 6.2. (a) CMOS microcoil array IC prototype. **(b)** CMOS/Microfluidic hybrid system prototype using the CMOS chip of Figure 2(a).

Building upon this experimental foundation that demonstrated the "move" capability of the hybrid system, we set our research goal at incorporation of a "see (detect)" capability into the hybrid system. The microcoils used for manipulation of bead-bound cells readily lend themselves to detection of the bead-bound cells. This is because a

magnetic bead, if placed at the center of the microcoil on the chip surface, changes the resonance characteristics of the microcoil, which can be detected by measuring the RF response of the microcoil. Development of an RF IC in CMOS that performs the on-chip RF measurement of the microcoil's resonance characteristic lies at the heart of this project.

Figure 6.3 shows the schematic of a proposed CMOS RF IC built around a microcoil, which measures the resonance characteristic of the microcoil. Two local oscillators (sine and cosine) generate low-phase noise RF signals, which are used to excite the microcoil. The homodyning of the response signal from the microcoil will yield information on the microcoil's resonance characteristic. By monitoring the microcoil response, one can sense a bead-bound cell because the magnetic bead will change the resonance characteristic (inductance) of the microcoil. Since the inductance change due to the magnetic bead is very small (0.1 ~ 1%), the important focus of this research was on increasing the sensitivity of the RF receiver via architectural, topological, and device-level design optimization.

Accomplishments: The proposed goal has been pursued in collobration with **Robert M**.

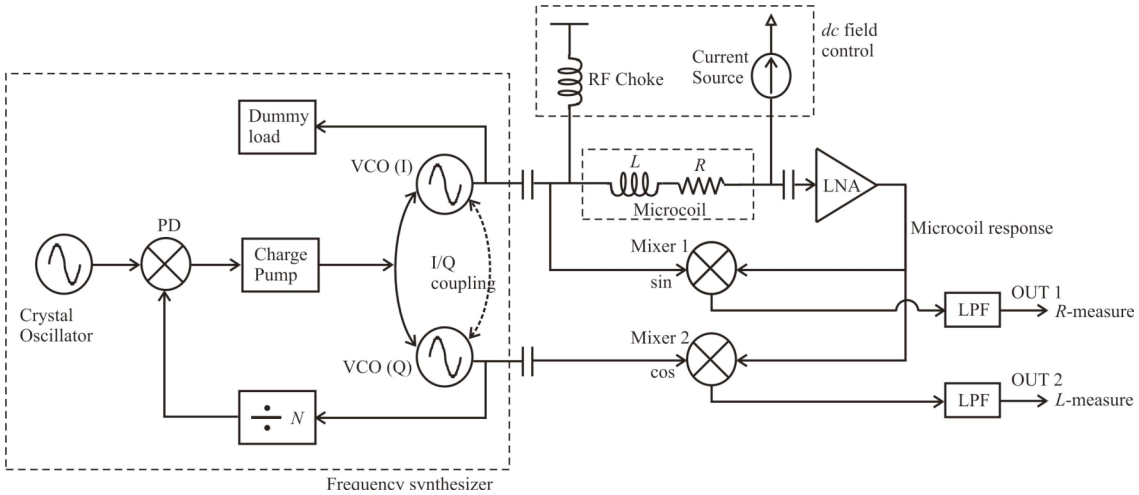

Figure 6.3. RF electronics with the microcoil for the RF sensing of a bead-bound-cell.

Westervelt (participating student in the **Donhee Ham** group: Yong Liu, G3). To attain the high sensitivity of the homodyning system, it is essential to reduce the phase noise of the local oscillators (the sine and cosine generators), by placing them in a phased-locked loop and minimizing frequency errors in the phase-locked loop (PLL). To this end, we developed an autonomic PLL that dynamically self-measures its jitters as well as mismatches and dynamically self-calibrates its loop parameters based upon the measurement data.

Figure 6.4 shows the schematic of the overall architecture of the self-calibrating autonomic PLL. In the charge pump PLL that is built around the voltage-controlled oscillator (VCO), the parameters of all the analog components such as loop filters, charge pumps, and voltage-controlled oscillators are dynamically adjusted by the digital control logic circuits. The digital control logic circuits are connected to jitter detectors, lock detectors, and phase offset detectors. These detectors self-measure the system jitter, lock status, and phase offsets, to give feed back signals for the digital control units. The

simulation of the overall system utilizing Cadence SpectreRF behavioral simulation tools attested to the validity of the proposed approach in minimizing the long-term frequency error as well as the short-term frequency instability (jitters). The overall system design was submitted to IBM foundry last fall, and we received the fabricated chip this spring. The chip testing is currently in progress.

Significance: When the RF sensor is used with the microcoil array, the RF sensor allows imaging of 2-D distribution of bead-bound-cells, where a single microcoil can be thought of as a "pixel". This imaging capability may render bulky optics unnecessary, realizing a

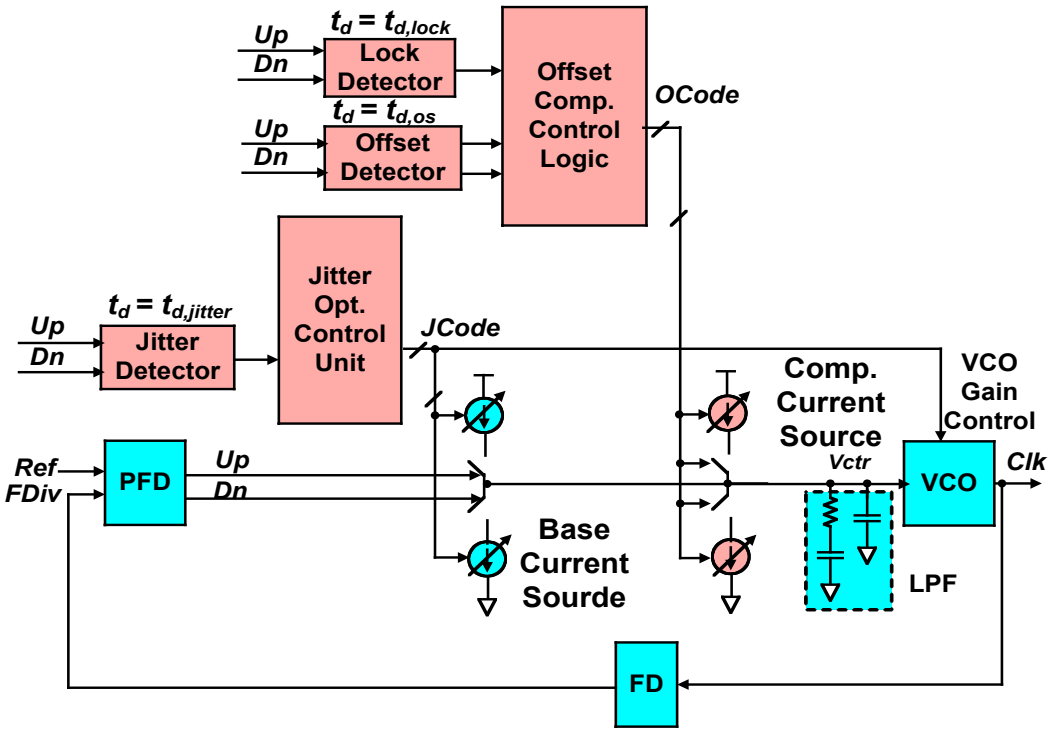

Figure 6.4: Self-calibrating autonomic PLL system architecture.

true lab-on-a-chip system. Additionally, the RF system may permit sensing of nanomagnetic beads too small to be seen optically. The RF sensor will offer a purely electrical way of sensing cells, not requiring chemical or optical methods. This project is aligned with the goal of Research Cluster 1 of the NSEC, which is aimed at the development of powerful new tools for manipulating and testing biological cells and tissues as nanoscale systems.

References

H. Lee *et al.*, "An IC/Microfluidic hybrid microsystem for 2-D magnetic manipulation of individual biological cells," *IEEE International Solid-State Circuits Conference* (2005).

H. Lee *et al.*, "IC/Microfluidic hybrid system for magnetic manipulation of biological cells," to appear in *IEEE Journal of Solid-State Circuits (JSSC)* (June 2006).

Y. Liu *et al.*, "IC/Microfluidic hybrid system for biology: Review" (Invited), *Proc. IEEE Bipolar/BiCMOS Tech. Meeting (BCTM)*, pp. 174–179 (Oct. 2005).

Silica Nanowires for Microphotonic Devices

Eric Mazur
Applied Physics and Physics, Harvard University
Collaborator: Federico Capasso (Harvard)

Silica nanowires provide strong mode confinement in a simple cylindrical silica-core/air-cladding geometry, representing a model system for the study of the nonlinear propagation of short pulses inside fibers. We observed supercontinuum generation by femtosecond laser pulses in silica fiber tapers of minimum diameters as small as 90 nm. This research was presented at the Photonics West 2006 Conference and a manuscript discussing supercontinuum generation in silica nanowires is currently being prepared.

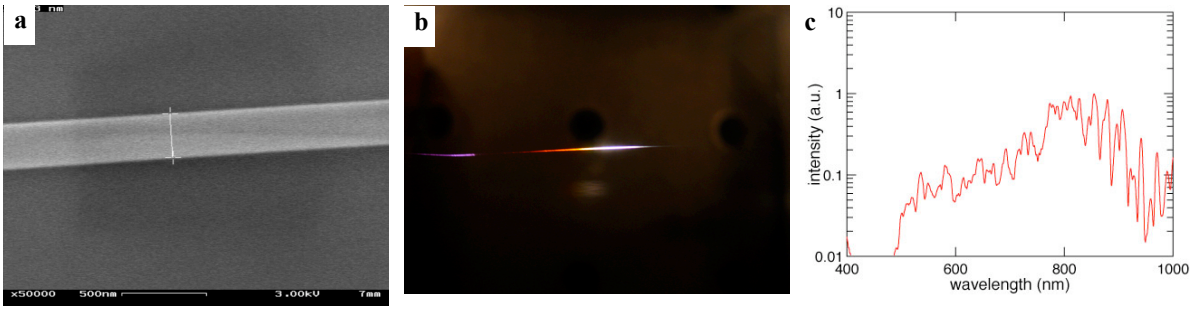

Figure 6.5. **(a)** Scanning electron micrograph of a 260-nm diameter silica wire. **(b)** Photograph and **(c)** spectrum of supercontinuum generation in a 526-nm average diameter silica wire.

Supercontinuum generation refers to extreme spectral broadening of a laser pulse propagating in a nonlinear material. Figure 6.5 shows a typical silica nanowire as well as the visual and spectral evidence of supercontinuum generation. Qualitatively, the degree of broadening of the supercontinuum spectra is understood in terms of the diameter-dependent dispersion and nonlinearity of the fiber. Contrary to supercontinuum generation by nanosecond pulses, for laser pulses propagating in negative dispersion regime, the observed spectrum is consistent with higher-order soliton formation and break-up. Because of the reduction of the interaction length to ~20 mm, and the low energy thresholds supercontinuum generation in tapered fibers is a viable solution for coherent white-light source in nanophotonics. Additionally, sub-200-nm diameter fibers possess negligible dispersion and nonlinearity making these fibers ideal media for propagation of intense, short pulses with minimal distortion.

The low threshold energies required to generate supercontinuum indicate that microphotonic devices can be constructed that take advantage of these nonlinear effects. Thus our current research efforts use subwavelength-diameter silica nanowires for the assembly of highly miniaturized photonics devices. Specifically, we plan to manufacture fundamental optical components such as one-to-many splitters, Sagnac interferometers, and nonlinear switches. These components allow efficient parallel assemblies to be produced, significantly reduce the interaction length required for nonlinear phenomena, and create possibilities for optical logic operations and computation. Our efficient and w-

cost technique opens the door to miniaturizing signal-processing nodes to a scale never achieved before.

Immunomodulating Nano-Platforms for Combatting Lung Infection

Joseph Mizgerd
Biology and Public Health, Harvard University
Collaborator: George M. Whitesides (Chemistry, Harvard)

Manipulating innate immune responses during infection will allow us to maximize antimicrobial efficacy while minimizing bystander tissue damage. Innate immune responses depend on polyvalent molecular interactions. We propose to develop tools for manipulating innate immunity in the lungs, in which molecules binding microbial surfaces or host cell receptors will function as immunomodulating agents when they are presented by nanomaterial scaffolds facilitating polyvalent interactions.

Polyvalency enhances avidity of adhesion, useful for targeting nanomaterials to cells, microbes, or tissues. Polyvalency cross-links receptors, sufficient to generate intracellular signaling cascades. For these reasons, otherwise inactive small molecules may become functional when presented on nanoscaffolds. Furthermore, platforms presenting multiple different small molecules can generate unique functionalities, eliciting distinct signaling cascades or cellular attachments. A variety of nanoscaffolding materials may be useful for such purposes, including polymers (e.g., of acrylamide) and solids (e.g., of gold), and the functionality of such nanoscaffolds may be determined in part by properties of the nanoscaffold including size, shape, and surface chemistry. Our long-term goal is to design and test new nanoscale tools for amplifying lung innate immune responses when and where they mediate antimicrobial host defense while dampening these responses when and where they cause inflammatory injury. We envision nanomaterials (i) mediating the ingestion and killing of bacteria by phagocytes, (ii) enhancing the

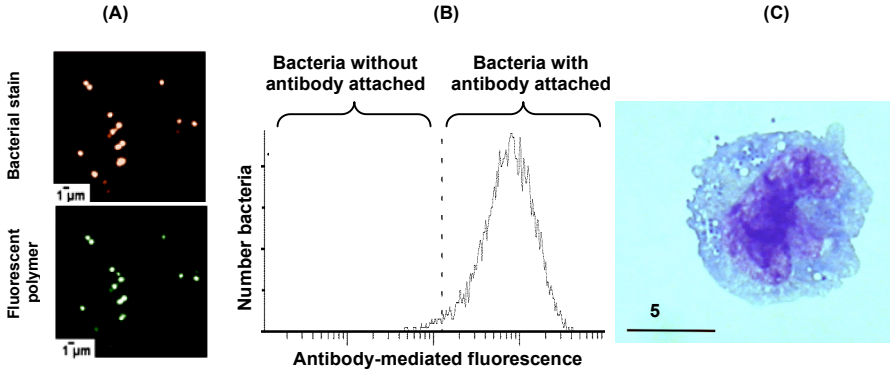

Figure 6.6. Nanomaterial targeting bacteria for phagocytosis. **(A)** Bacteria, stained red, are coated with polymer, fluorescing green. **(B)** Polymer-coated bacteria become painted with antibody. **(C)** A macrophage (~10 µm diameter) ingesting polymer-coated antibody-painted bacteria (dark blue spheres of <1 µm).

recruitment and activation of phagocytes in the lung, and (iii) protecting lung cells from inflammatory damage.

During the first year of our participation in the NSEC, we have demonstrated proof of principle for the first of these concepts (nanomaterials mediating phagocytosis), as demonstrated in our upcoming publication. Together with **George M. Whitesides**, we observe that nanomaterials presenting 2 moieties, 1 targeting a structure common to Gram-positive bacterial cell walls and the other targeting antibodies, can induce phagocytosis of bacteria. In short, we use a nanomaterial (in this case 100-nm polyacrylamide polymers, but other materials may be equally or more efficacious) to coat bacteria with an antigen, and then we opsonize the bacteria by adding antibody against that antigen. Phagocytic immune cells recognize antibody-opsonized bacteria and ingest them. We can use this strategy to opsonize diverse Gram-positive bacteria. For some bacteria, such as *Staphylococcus aureus*, this induces phagocytosis (Figure 6.6).

Although these polymers were effective at improving phagocytosis of bacteria *in vitro*, they were ineffective when tested in living animals. A goal for the upcoming year is to determine whether simpler (monofunctional rather than bifunctional) polymers are capable of inducing biological responses in the lungs. This will involve the design, synthesis, and testing of a distinct set of polymers, presenting in a multivalent fashion a small molecule known to signal to lung cells. These new polymers will be tested *in vivo* and compared to a comparable dose of monomers. These experiments will help determine whether polymer nanostructures are useful platforms for exploiting polyvalency as a therapeutic avenue in the lungs.

A new goal for this year is to begin designing nanomaterials for the recruitment and activation of phagocytes. We have molecular targets in mind, and we are meeting with **George M. Whitesides** and his group to discuss molecules of interest, chemical screening approaches, nanomaterials for scaffolding, and synthesis feasibility. Our goals for the upcoming year are (i) to identify molecules binding to receptors of interest yet small enough to be useful on nanoplatforms, (ii) to present these molecules on nanostructures for polyvalent interactions, and (iii) to determine whether polyvalent interactions induce intracellular signaling from the receptors of interest. Ensuing experiments will test the efficacy of these novel nanomaterials in improving host defenses during experimental pneumonias in mice.

Nonmechanical Regulators of Cardiac Bioelectricity

Kevin (Kit) Parker
Bioengineering, Harvard University
Collaborator: Robert M. Westervelt (Harvard)

We have made great progress in the last year on several projects that are supported by the NSEC and NSEC core facilities.

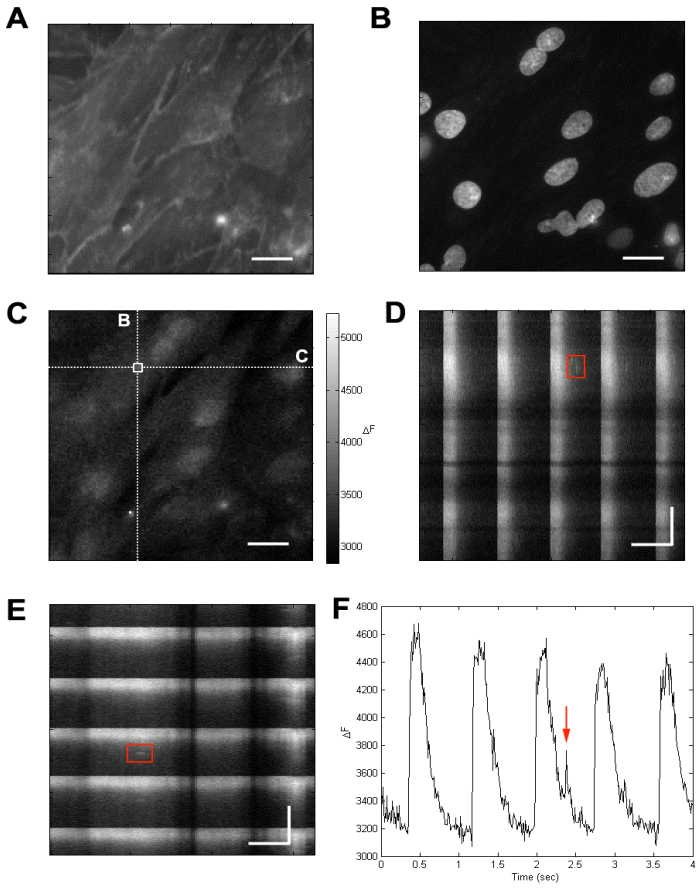

Figure 6.7. Example of raw fluorescence data obtained by a CCD camera from an engineered two-dimensional sheet of cardiac myocytes. (A-C). A single (x,y) fluorescence map taken at t = 2.38 sec labeled with (A) di-8-ANEPPS, highlighting the myocyte membranes, (B) DAPI, highlighting the nuclei, and (C) fluo-4, showing $[Ca^{2+}]_i$. (D,E) Development in time of DF along the dotted lines labeled D and E shown in (C). The red boxes outline the same spark in (D) and (E). The periodic pattern represents spontaneous Ca^{2+} transients that occupy the entire tissue area simultaneously. (F) Temporal trace at the location shown in (C) with a white box, illustrating the spontaneous Ca^{2+} transients and the spark highlighted in (D) and (E) indicated by a red arrow. Scale bars in (A-C), vertical scale bar in (D) and horizontal scale bar in (E) are 20 mm, horizontal and vertical scale bar in (D) and (E) are 0.5 sec.

Calcium Sparks. We are studying the structure function relationships that potentiate Ca^{2+} sparks, the opening of single ion channels on the membrane of a cardiac myocyte, and their coupling to single sarcoplasmic reticulum by diffusion of Ca^{2+} in the sub-micron space separating the two structures. Sparks are important because these discrete events sum to a Ca^{2+} wave during excitation-contraction coupling in the heart. We have developed new algorithms for detecting these events (Bray, Geisse, and **Parker**, submitted) and continue our experimental studies of sparks in engineered cardiac myocytes (Figure 6.7).

Cellular Nanosurgery. A new project in our laboratory is the development of an experimental system for image-guided cell nanosurgery. In this setup, we have coupled an atomic force microscope (AFM) to an inverted optical microscope with a high-speed camera capable of fluorescent video microscopy. We are currently developing nanoscale surgical instruments for the AFM tip that will allow us to conduct invasive operations on living cells, grab, move, and deposit single proteins or cell organelles (Figure 6.8). This involves focused ion beam machining of AFM tips for instrumentation (Figure 6.9). We anticipate that these engineering efforts will continue until we have constructed a system that will allow us to surgically assemble a customized cell.

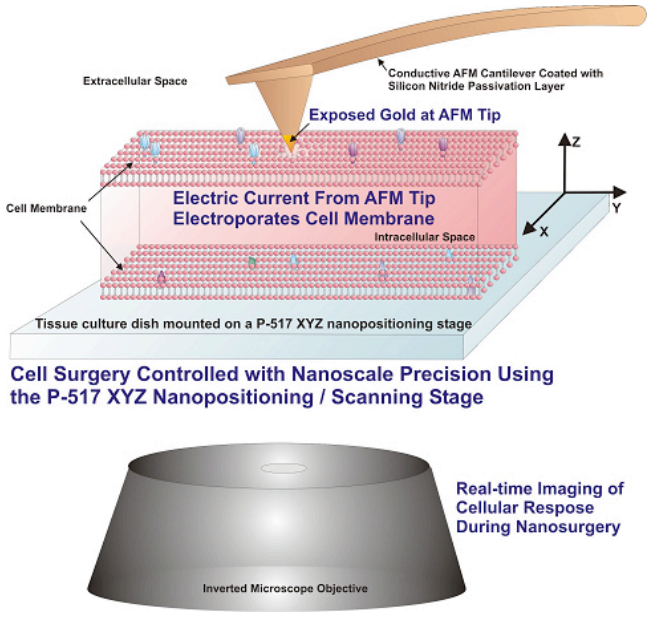

Figure 6.8. Schematic of AFM and LCSM setup with integrated PI Nanopositioning/Scanning Stage. Cells are adhered to specialized tissue culture dishes with glass bottoms, above a LSCM objective. A strong electric current applied to a conductive cantilever tip electroporates the cell membrane to form 80–200-nm diameter pores. The nanopositioning stage is utilized to control and automate the position of these pores, such that non-destructive nanoincisions can be made with enhanced precision. The cells can be loaded with fluorescently-tagged proteins, voltage sensitive dyes, or Ca^{2+} indicators to obtain real-time images of alterations in cell physiology during nanosurgery.

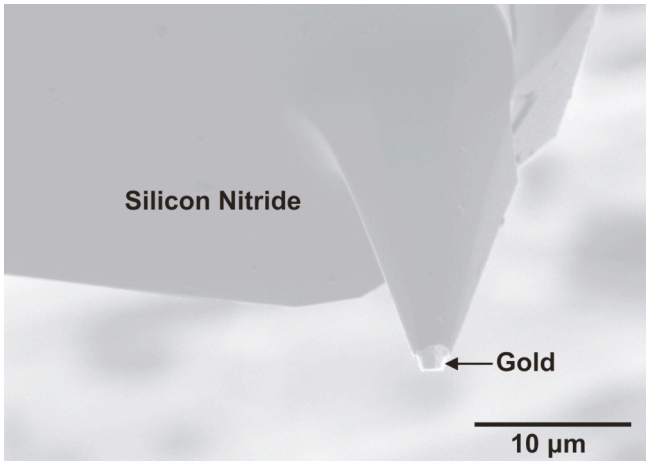

Figure 6.9. SEM image (6.50 kX magnification) of a conductive AFM cantilever tip. The silicon AFM cantilever is patterned with a 10-nm thick chrome layer and a 300-nm thick gold layer, and insulated with a 300-nm thick silicon nitride passivation layer. Selective etching at the cantilever tip exposes the underlying gold layer, allowing for local delivery of current during electroporation experiments.

Development and Characterization of a Cellular-Scale Differential Manometer Modelling of an Artificial Flagella

Howard A. Stone
Materials & Fluid Mechanics, Harvard University
Collaborator: J. Bibette (ESPCI, Paris), George M. Whitesides (Harvard)

We have pursued two distinct areas of research for the NSEC: (i) *Development and characterization of a cellular-scale differential manometer* (reported in *PNAS* 2006) and (ii) *Modelling of an artificial flagella* (reported in *Nature* 2005). Both projects are part of the NSEC effort in *Tools for Integrated Nanobiology*. The projects have engaged undergraduates. Also, the research has included experimental contributions and theoretical and numerical advances.

In the first project we have designed a new approach to probe the mechanical response of cells under continuous flow conditions. Since most if not all existing mechanical measurements on individual cells examine cells that are stationary on substrates, the opportunity to investigate, even qualitatively, the mechanical response for cells flowing continuously through a device may offer new ideas in cellular-scale sensing.

In the second project we have collaborated on what is likely the first micron-scale flagella-like element which can swim in controlled directions.

1. *Development and characterization of a cellular-scale differential manometer*: It is known that the mechanical properties of cells are linked to some diseases (e.g., malaria). In addition, chemicals are known to affect the mechanical response of cells. We have developed a microfluidic device with dimensions comparable to individual red blood cells, which provides an indication of the change of pressure when the cell enters the smallest channel (see Figures 6.10a, b). The methodology in principles works for any kind of small or flexible object and has a time resolution on the order

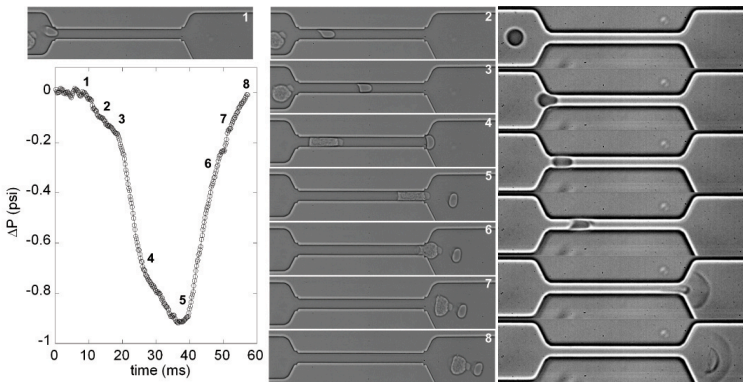

(a) **(b)** **(c)**

Figure 6.10. (**a)–(b)**. Entry of a red blood cell, followed by a white blood cell, into a narrow channel with dimensions comparable to the cell. The pressure change recorded using the manometer we have developed is shown. **(c)** Flow of a swollen red blood cell into a narrow channel; lysis occurs.

of milliseconds. The measurement can be performed even when cells undergo lysis (see Figure 6.10c) and can distinguish cells that have been made more rigid by addition of gluteraldehyde. These results suggest that this continuous flow approach to sensing changes in mechanical properties of cells can be accomplished and combined with the flexibility of microfluidic approaches for controlling chemical composition. We are currently pursuing several new directions of this project. More recent work has included the development of numerical simulation tools for these kind of flow situations and additional controlled experiments probing the influence of chemicals on the mechanical response of the cells.

2. *Modelling of an artificial flagella*: In a collaboration with the group of J. Bibette (ESPCI, Paris) we studied the first artificial flagella ever created. The Paris group created the object and experimentally demonstrated the idea and we developed a continuum description of the magneto-elastic filament. The micron-length slender elastic object consists of magnetic nanometer-diameter spheres tied together using DNA and biotin-streptavidin links. The slender filament can be aligned along the direction of a constant externally applied magnetic field. Application of a transverse magnetic field causes a wave to travel along the filament and if fore-aft symmetry is broken, the filament swims. Symmetry breaking was shown to happen naturally owing to inevitable defects, or could be produced by tying the filament to a large object. By attaching the filament to a red blood cell, the cell could be transported in a controlled fashion.

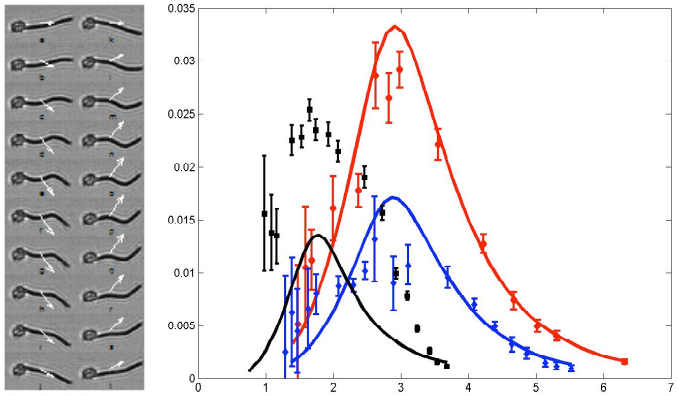

(a) **(b)**

Figure 6.11. **(a)** Sequence of deformation of the end of a free filament. The propagation of a bending wave is indicated by the arrows. Conditions for the magnetic field: $B_x = 9$ mT, $B_y = 14$ mT, $f = 20$ Hz. Each image corresponds to pictures taken every 2.5 ms. Length of the portion of the filament shown: 34 µm. **(b)** Scaled velocity as a function of

$$S_p = L / \left(\frac{\kappa}{4\pi\eta\omega} \right)^{1/4}.$$

Experimental data are discrete points while the continuous lines are the predictions obtained with our model. Error bars are calculated by measuring the drift velocity of a filament when the transverse magnetic field $B_y = 0$ and by estimating the standard deviation of the bending modulus. The cell radius a_s and the distance a_l of the attachment point from the cell center are evaluated from experimental images.

Black squares: Bending modulus $k = 3.3.10^{-22}$ J.m, $L = 13$ µm, $B_x = 8.7$ mT, $B_y = 9.3$ mT, $a_s = 3.2$ µm, $a_l = 3.2$ µm. *Blue diamonds*: $k = 3.3.10^{-22}$ J.m, $L = 21$ µm, $B_x = 8.7$ mT, $B_y = 9.3$ mT, $a_s = 2.7$ µm, $a_l = 0$ µm. *Red circles*: $k = 3.3.10^{-22}$ J.m, $L = 24$ µm, $B_x = 8.9$ mT, $B_y = 10.3$ mT, $a_s = 3.1$ µm, $a_l = 3.1$ µm.

Hybrid CMOS / Microfluidic Micropost Array for Manipulation of Biological Systems using Dielectrophoresis (DEP)

Robert M. Westervelt
Applied Physics and Physics, Harvard University
Faculty Collaborator: Donhee Ham
Outside Collaborators: Rick Rogers (Harvard School of Public Health) and Giannoula Klement (Harvard Medical School)

In collaboration with **Donhee Ham**, we have developed hybrid CMOS/Microfluidic chips that combine the power of integrated circuits with the biocompatibility of microfluidic systems. In previous work (Lee *et al.*, 2005), we fabricated and tested two generations of hybrid chips that used a two-dimensional array of microcoils to manipulate cells tagged with magnetic beads in the microfluidic system above. A custom-built integrated circuit made in a foundry contains the microcoil array, along with integrated current and control circuits. The microfluidic system is fabricated on top of the IC at Harvard. Tests using an optical microscope show that the hybrid chip can trap and move a magnetic bead, and the attached cell, through the fluid. By energizing more than one microcoil, many beads can be independently manipulated at the same time. An excellent description of this approach is given in **Donhee Ham**'s description of his plans. This research has attracted a number of invited talks, including one for Hakho Lee at last year's IEEE Integrated Solid State Circuits Conference (ISSCC) in San Francisco, as well as an invitation for Hakho Lee, **Donhee Ham**, and myself to edit a book titled *BioCMOS* in the series *Integrated Circuits and Systems* (series editor Prof. Chandrakasan).

Tom Hunt has developed an analogous bio chip based on RF electric fields, shown in Figure 6.12, that uses dielectrophoresis to trap and move cells and other dielectric objects. For his home-made version, Tom built a two-dimensional array of microposts using lithography at Harvard, then made a microfluidic 'bathtub' on top with an electrically conducting top plate. By applying an RF (1–10 MHz) voltage between one of the microposts and the top plate, an object with higher dielectric constant than the fluid can be attracted and trapped. By sequentially

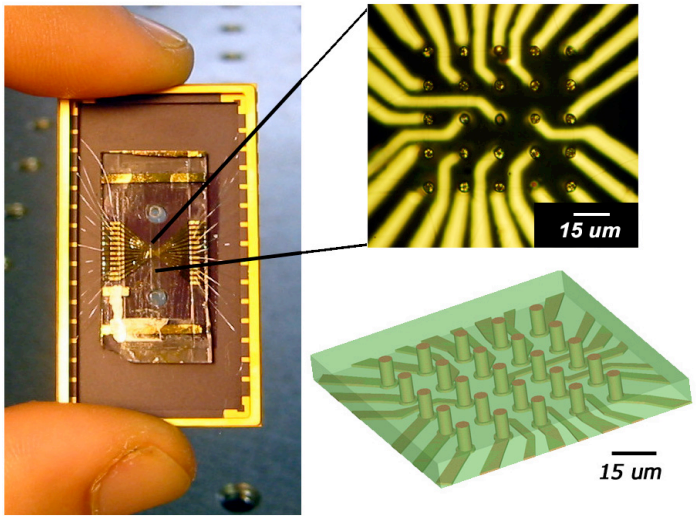

Figure 6.12. Two-dimensional micropost array for the manipulation of small objects in a microfluidic system using dielectrophoresis (Hunt *et al.,* 2004).

changing which micropost is energized, the location of the trapped object can be moved through the fluid. This approach works very well, and was used to move yeast cells (positive DEP) as well as polystyrene beads (negative DEP) (Hunt *et al*., 2004).

Tom Hunt plans to extend this approach by developing a hybrid CMOS/Microfluidic chip to manipulate objects in a fluid using dielectrophoresis. The overall concept is similar to the magnetic manipulator chip described above, except that a two-dimensional micropost array replaces the microcoil array, and spatially patterned electric fields replace the magnetic fields. The two-dimensional micropost array is analogous to a flat panel digital display in which each pixel is represented by a micropost. Using current integrated circuit technology, it is possible to make large arrays with integrated RF sources and control circuits. One can then create a region for trapping an object that has the right size and shape, much as one displays a picture on a microcomputer display. A microfluidic system built on top of the IC provides a biocompatible environment.

The hybrid CMOS/Microfludic DEP chip will allow us to trap and move small objects in a fluid without using magnetic beads for tagging. This approach works for biological cells, although relatively large electric fields can cause electroporation of cell walls, limiting their life. The hybrid DEP chip can also be used to trap, move and assemble small inorganic objects in a fluid. This may provide a way to assemble nanoscale building blocks such as semiconductor nanowires into systems and circuits. In that case a custom array fabricated using e-beam lithography may be necessary.

References

T. P. Hunt, H. Lee and R.M. Westervelt, "Addressable micropost array for the dielectrophoretic manipulation of particles in fluid," *Appl. Phys. Lett*. **85**, 6421 (2004).

Hakho Lee, Yong Liu, Eben Alsberg, Donald E. Ingber, R.M. Westervelt,and Donhee Ham, "An IC/Microfluidic Hybrid Microsystem for 2-D Magnetic Manipulation of Individual Biological Cells," IEEE Int. Solid State Circuits Conference, *ISSCC Dig. Tech. Papers*, 80–81 (2005).

Nano-and Microscale Tools for Use in Molecular and Cell Biology

George M. Whitesides
Chemistry, Harvard University
Collaborators: Howard A. Stone, Joseph Mizgerd (Harvard)

Summary. We are preparing nano- and microscale tools for use in molecular and cell biology. The characteristic of these tools is that they must be simple enough that they can be fabricated and used by *biologists*: Systems that require the capabilities of an electrical engineer are too complicated to be useful. They must also meet the stringent requirements of biocompatibility that characterize biological systems.

Gradients in Biological Active Materials on Surfaces. We have developed a procedure based on a microfluidic system to make gradients of arbitrary biomolecules on surfaces. This procedure starts from microfluidic methods developed earlier, and adapts them to make gradients in the molecule biotin. This molecule binds essentially irreversibly to the tetrameric proteins avidin and streptavidin, but leaves binding sites

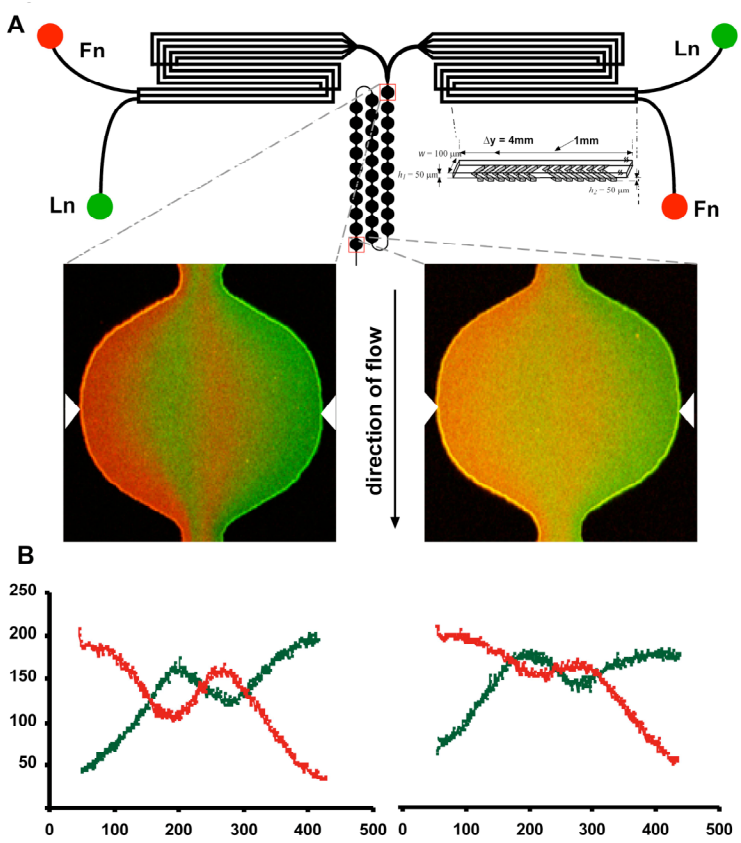

Figure 6.13. We combined overlapping gradients of laminin (Ln) and fibronectin (Fn) into complex contours: **(A)** illustrates the design of the μFN. Anti-Fn (mouse) and anti-Ln (rabbit) were used as primary antibodies, and anti-mouse-fluorescein and anti-rabbit-Texas red were used as secondary antibodies to visualize these gradients. Arrowheads point to the axis along which of fluorescence intensity was read. **(B)** Fluorescence intensities as functions of the distance across the channel. (from Jiang *et al.* (2005)).

vacant. Exposure of this surface—with what is now a gradient in avidin—to a solution of a protein (or other biomolecule of interest) to which biotin has been covalently linked generates excellent gradients. Since this method is both structurally familiar to biologists, and very general, it should provide a very useful method for studying problems in which gradients of this type are needed for studying, for example, chemotaxis as an influence in cell motility.

Fluorescent, On-chip Light Source. Most detection methods for use on-chip are based on optical methods. In a typical experimental protocol, an off-chip light source (for example, a laser) is used to irradiate a micro/nano sample of interest, and the reflected or adsorbed light is analyzed by a detector operating off-chip. In some types of experiments, this arrangement of off-chip generation and detection of light is appropriate; in others, it is not. We have been interested in developing on-chip light sources and detectors. In the first parts of this work to be published, we have demonstrated the design and fabrication of a channel system which—when filled with a fluorescent dye and illuminated with UV light—emits light. The intensity of light emitted along the axis of the channel is sufficiently strong to provide a good on-chip light source. In subsequent work, we have extended this methodology to build a complete on-chip microfluidic laser, and have demonstrated that this system give good amplification and excellent linewidth–~ 2 nm—when operating on-chip.

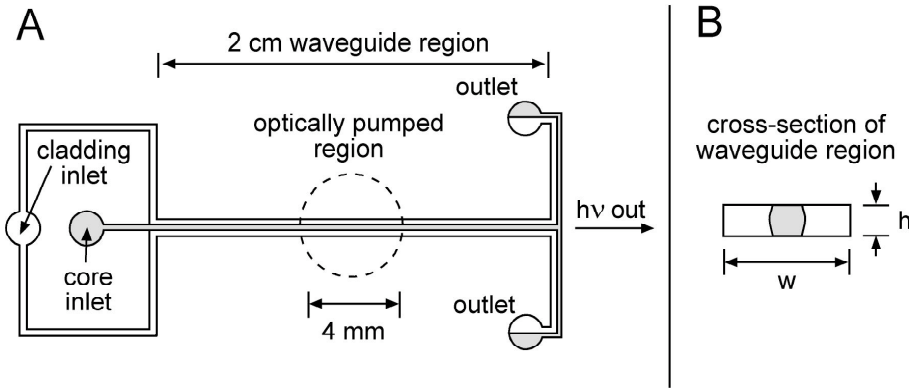

Figure 6.14. (A) Top-view scheme for the L^2 fluorescent light source based on microfluidic channels in PDMS. **(B)** The cross section of the device that was used for imaging onto the photodiode and CCD camera was 50 μm x 200 μm (h x w). Larger microchannels – 125 μm x 500 μm (h x w) – were used for end-coupling the device to a spectrometer with optical fiber (125 μm outer diameter). (from Vezenov *et al*. (2005))

Thin, Metallic Wires with Electrical Connections. One of the prototypical problems in cell biology is to develop methods for making electrically connected wires that have nanometer-scale widths, and that sit in the plane of the support to which cells are attached. We have developed a first step toward such a system using an adaptation of a system reported by Rogers *et al.,* in which the metal (typically gold) is deposited on a contoured surface, and then the gold in the top-most surfaces is removed by a mechanical process. The trench can, if desired, be filled with polymer to leave only the exposed edges of the wires exposed—these can have widths down to approximately 20 nm.

Methods for Nanotechnology. We have developed a new, sacrificial polymer system based on poly(acrylic acid) (PAA) and other negatively charged polymers. The key feature of this system is that the polymer can be rendered essentially insoluble in water by exposing it to a variety of di- and tri-valent ions (for example, Ca^{+2} or Ho^{+3}). These metal-crosslinked films are quite insoluble in water, and serve as a stable basis for fabrication of other structures. Treating them with an aqueous solution of EDTA (ethylene diamine tetraacetic acid) removes the cross-linking ions, and allows the PAA to dissolve under very mild conditions in water.

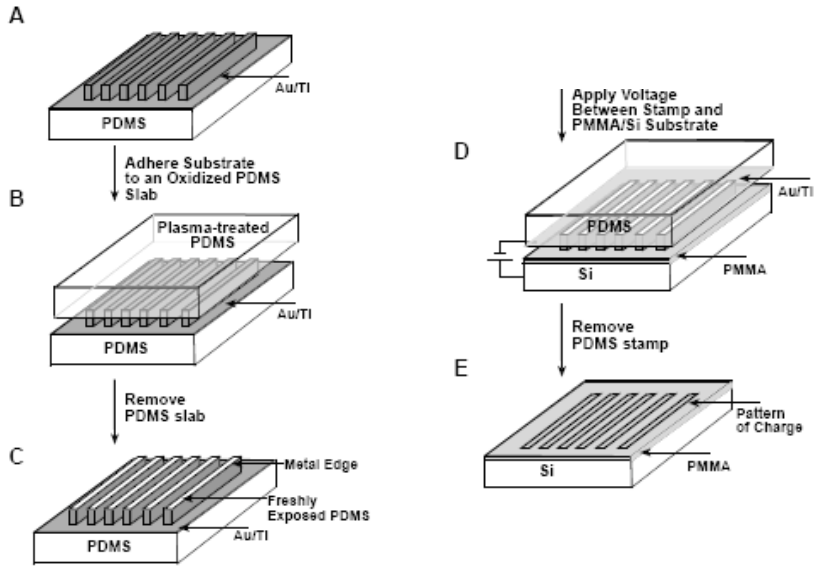

Figure 6.15. A schematic representation outlining each step of the procedure of fabricating a PDMS stamp with thin, metallic edges using nTP, and of performing e-μCP with this stamp. **(A–C)** A PDMS stamp fabricated by soft lithography coated with a thin film of Au followed by a layer of Ti, conformally contacts a flat, oxidized PDMS to remove the metal film from the raised features of the stamp. **(D–E)** A voltage applied between the PDMS stamp with the remaining, conducting metal edges and a dielectric thin film embeds a pattern of charge in the thin film that corresponds to the outline of the relief features of the PDMS stamp(from Cao *et al.* (2005)).

We have also developed methods of looking at biologically relevant electron transfer reactions in ultrathin layers of electrolyte solution in contact with ultrathin organic membranes (self-assembled monolayers or SAMs).

References

Cao, T., Xu, Q., Qinkleman, A., and Whitesides, G.M., "Fabrication of thin meallic films along the sidewalls of a topographically patterned stamp and their application in charge printing," *SMALL* **1**, 1191–1195 (2005).

Gates, B.D., Xu, Q., Stewart, M., Ryan, D., Willson, C.G., and Whitesides, "New approaches to nanofabriccation: Molding, printing and other techniques," *Chem. Rev.* **105**, 1171–1196 (2005)

Jiang, X., Xu, Q., Dertinger, S.K.W., Stroock, A.D., Fu, T., and Whitesides, G.M., "A general method for patterning gradients of biomolecules on surfaces using microfluidic networks," *Anal. Chem.* **77**, 2338–2347 (2005).

Linder, V., Gates, B.D. Ryan, D., Parviz, B.A., and Whitesides, G.M., "Water-soluble sacrificial layers for surface micromachining," *SMALL* **1**, 730–736 (2005).
Tran, E., Whitesides, G.M. and Rampi, M.A., "Controlling the electron transfer mechanism in metal-molecules-metal junctions," *Electrochimica Acta* **50**, 4850–4856 (2005).
Vezenov, D.V., Mayers, B.T., Wolfe, D.B., and Whitesides, G. M., "Integrated fluorescent light source for optofluidic applications," *Applied Physics Letters* **86**, 041104-1–041104-3 (2005).

Developing Highly Fluorescent and Raman-active Silver Nanocrystals as New Bio-labels for Live Cell Imaging

Xiaowei Zhuang
Chemistry and Physics, Harvard University
Collaborator: Charles M. Lieber (Harvard)

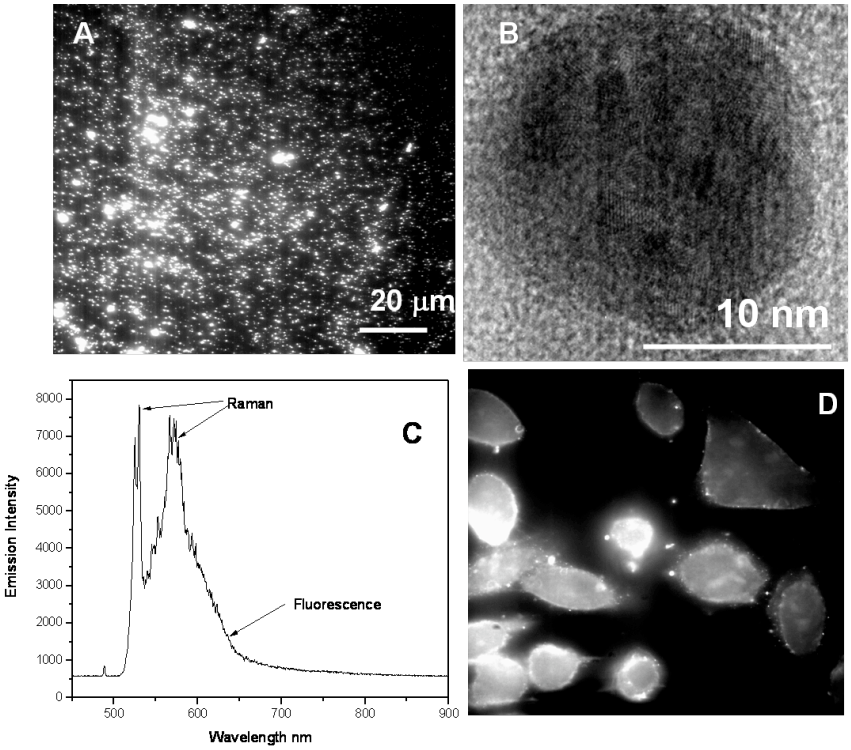

Figure 6.16. Fluorescent and Raman active silver superclusters**. (A)** Fluorescence and Raman image of silver superclusters. **(B)** High resolution TEM image of a single silver supercluster. **(C)** A Fluorescence and Raman spectrum of silver superclusters. **(D)** Fluorescence image of fixed HeLa cells labeled with silver superclusters.

A grand challenge in biological imaging is to develop tools for imaging individual biomolecules and their interactions *in vivo* with high spatial and temporal resolution. While highly luminescent semiconductor quantum dots overcome limitations of organic dyes or fluorescent proteins on photostability and emission intensity, these fluorescence based quantum dots are toxic and provide little chemical information on the interactions

of biomolecules with surroundings. Consequently, a fluorescent label with giant Raman enhancement function potentially offers a new dimension to meeting this challenge. As a part of the *Cluster 1 — Tools for Integrated Nanobiology*, we propose to develop highly fluorescent and Raman-active silver superclusters as a new type of biolabel and to use them for tracking individual molecules in living systems and for chemical (Raman) sensing their chemical interactions with the surroundings.

Noble metals exhibit a particularly wide range of material behavior along the atom to bulk transition. As a special state of noble metals on the nanoscale, superclusters are polycristalline nanoparticles made of very small metal nanocrystals whose sizes are comparable to Fermi wavelength of an electron. Recently, we were able to create biocompatible and monodisperse silver superclusters with sizes around tens of nanometers which exhibit not only single particle fluorescence as bright as quantum dots but also enormous Raman enhancement with factors on the order of 10^{14}–10^{15} (Figure 6.16A–C). Preliminary data also show that these superclusters indeed could be used as biolabels. They are compatible with cellular imaging and show high photo and chemical stability without losing Raman activity in physiological conditions (Figure 6.16D).

In the next 1–2 years, we plan to accomplish the following aims:

1. Functionalize surface of these superclusters for specific labeling of biomolecules.
2. Use these superclusters as labels for tracking individual protein and RNA molecules in live cells.
3. Investigate the mechanism of Raman-enhancement effect of these silver nanocrystals. We will utilize this large Raman enhancement effect to detect distributions of drug molecules and metabolites in a living cell.

Cluster 2: Nanoscale Building Blocks

Period: March 16, 2005 to March 15, 2006

Coordinators: Moungi Bawendi and Hongkun Park

Moungi Bawendi (Chemistry, MIT)	Charles Lieber (Chemistry & DEAS, Harvard)
Federico Capasso (DEAS, Harvard)	Charles M. Marcus (Physics, Harvard)
Cynthia M. Friend (Chemistry & DEAS, Harvard)	Hongkun Park (Chemistry, Harvard)
Bertrand I. Halperin (Physics, Harvard)	Shriram Ramanathan (DEAS, Harvard)
Efthimios Kaxiras (Physics & DEAS, Harvard)	

International Collaborator(s): Lars Samuelson (Lund University, Sweden)

Number of postdoctoral fellows: 2
Number of graduate students: 5
Number of undergraduate students: 4

Introduction

Tremendous progress has been made in the synthesis of nanoscale structures – nanoparticles, nanowires and nanotubes – that serve as building blocks for new devices and applications. However many challenges remain. These include the synthesis of nanostructures with well-defined sizes and shapes, the synthesis of new classes of materials, the in-depth characterization of newly developed nanostructures, the rational organization of these nanostructures into complex functional structures, and the fusion of nanoscale building blocks with state-of-the-art processing techniques, including e-beam lithography and focused-ion-beam sculpting to build novel devices.

A broad multidisciplinary, multi-investigator research program is proposed that is designed to address these challenges. The proposed research is solidly built upon the participants' expertise on the synthesis and characterization (both experimental and theoretical) of nanostructured materials. At the core of the program is the ***rational synthesis of new classes of nanostructures that exhibit new size-dependent properties*** that are distinct from bulk materials, with an emphasis on semiconductor and metallic nanostructures with unconventional shape, as well as on zero-, one- and two-dimensional nanostructures based on new materials, including metal chalcogenides, that have not been made previously. The ***incorporation of nanostructures into novel device geometries*** will constitute another important part. These devices will be used to characterize the physical and chemical properties of nanoscale materials and to test their technological applicability. ***Understanding the behavior of these nanoscale building blocks*** through theoretical investigations will be an important part of the proposed efforts, because it is essential for furthering the scientific and technological frontiers of nanomaterials.

Major Accomplishments

The Semiconductor Industry Association (SIA) recently created the Nanoelectronics Research Institute (NRI) to support academic research for in the development of quantum

switches for ultrasmall electronics in the coming years. Our Center was selected for an NRI supplement for research in new oxide semiconductors that show promise for phase switches based on phase transitions. This will be carried out by Shriram Ramanathan, a new Harvard faculty member who recently arrived from Intel.

Lars Samuelson recently joined the Center as an international collaborator. Samuelson is a leading expert in the synthesis of new types of nanoscale structures. He is the Director of the Nanometer Structure Consortium at Lund University in Sweden.

Multifunctional Microspheres for Magnetic Manipulation and Fluorescent Tracking

Moungi G. Bawendi
Chemistry, Massachusetts Institute of Technology
Collaborator: Robert M. Westervelt (Harvard)

We present magnetic and fluorescent silica microspheres. These multifunctional particles were fabricated by incorporation of maghemite nanoparticles (MPs) and CdSe/CdZnS and CdS/CdZnS quantum dots (QDs) into a silica shell grown on preformed silica microspheres, as shown in Figure 6.17a. The QDs and MPs were chemically modified to be compatible with sol-gel chemistry. The shell was then grown in the presence of our modified MPs and QDs. The MP content in the microspheres was calculated from the saturation magnetization of microspheres obtained from a superconducting quantum interference device (SQUID). The morphology and size dispersity of the microspheres were observed by scanning electron microscopy (SEM) (Figures 6.17b, 6.17e) and transmission electron microscopy (TEM) (Figures 6.17c, 6.17f). The incorporation process did not affect the size dispersity of the microspheres (Figures 6.17d, 6.17g). Scanning transmission electron microscopy (STEM) (Figures 6.17h, 6.17i) revealed the MP distribution and the core-shell structure of the microspheres.

These magnetic and fluorescent microspheres were manipulated using magnetic field gradients created by microelectromagnetic devices, and simultaneously tracked in real-time by fluorescence microscopy, as shown in Figure 6.18. These multifunctional microspheres are promising for various applications in biomedical research and technology.

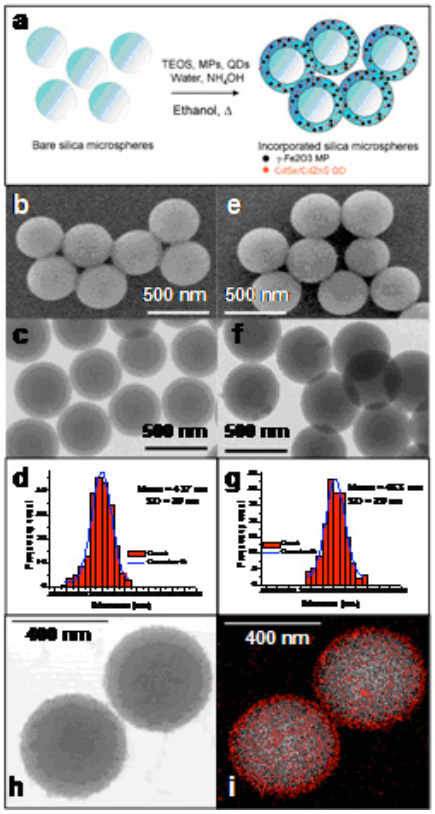

Figure 6.17. (a) Reaction scheme for the incorporation of silica microspheres. **(b-d)** 500-nm silica microsphere before incorporation (Polysciences, 500 ± 70 nm). **(b)** SEM image. **(c)** TEM image. **(d)** size distribution analysis. **(e–g)** 500-nm silica microspheres after incorporation of QDs and MPs (9 nm MP, 1145 MP per microsphere), **(e)** SEM image. **(f)** TEM image. **(g)** Size distribution analysis. **(h,i)** results from STEM. **(h)** Transmission image and **(i)** distribution map of silicon (white spots) and iron (red spots).

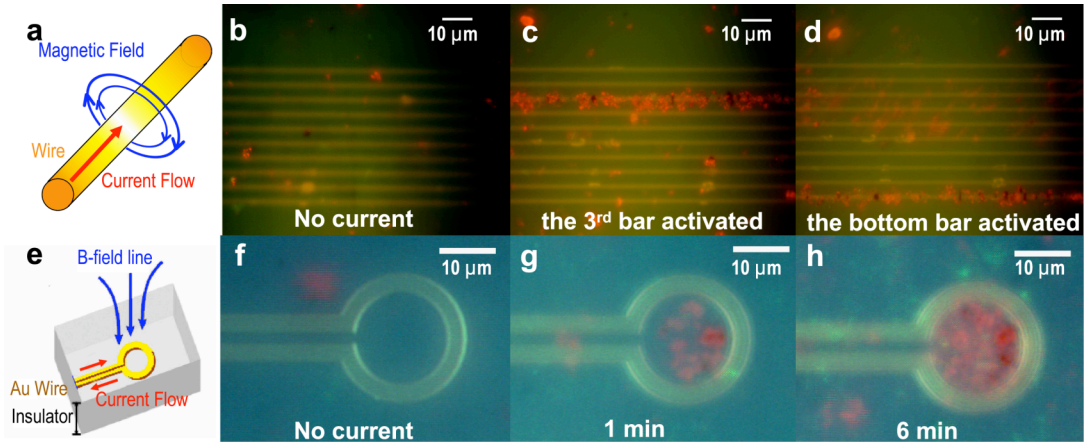

Figure 6.18. Images of **(a-d)** the straight wires trapping experiment, **(a)** the current flow and magnetic field from the wires, **(b)** no current in wires, **(c)** third wire from the top turned on, **(d)** bottom wire turned on, **(e-f)** the ring trapping experiment, **(e)** the current flow and magnetic field from the ring, **(f)** no current, **(g)** after the ring current was turned on for one minute, **(h)** after the ring current was turned on for six minutes.

Nanophotonic Devices

Federico Capasso
Applied Physics and Electrical Engineering, Harvard University
Collaborators: Charles M. Lieber (Harvard), Kenneth B. Crozier (Harvard)

During the last year **Capasso** and his group**,** in collaboration with **Charles Lieber** and his group, have initiated a nanophotonics program to explore the scaling limits of a variety of passive and active photonics components (gratings, cavities and resonators, light emitters). They have demonstrated a hybrid approach for photonic systems that combines chemically-synthesized single nanowire emitters with lithographically-defined photonic crystal and racetrack microresonator structures. These hybrid structures exploit unique strengths of bottom-up and top-down approaches and thereby open new opportunities in nanophotonics from efficient and localized light sources to integrated optical processing. Finite-difference time-domain (FDTD) calculations were used to design nanowire photonic crystal structures where the photonic band gap overlaps with the electronic band gap of the cadmium sulfide (CdS) nanowire. Photoluminescence imaging and spectroscopy of nanowire photonic crystal structures demonstrate localized emission in engineered artificial defects and light suppression in the region of the photonic crystal (Figure 6.19).

Capasso's and **Lieber**'s group have also used one-dimensional photonic crystal cavities to improve the reflectivity of the nanowire end facets. In addition, they spectroscopically investigated nanowire racetrack microresonators (Figure 6.19).

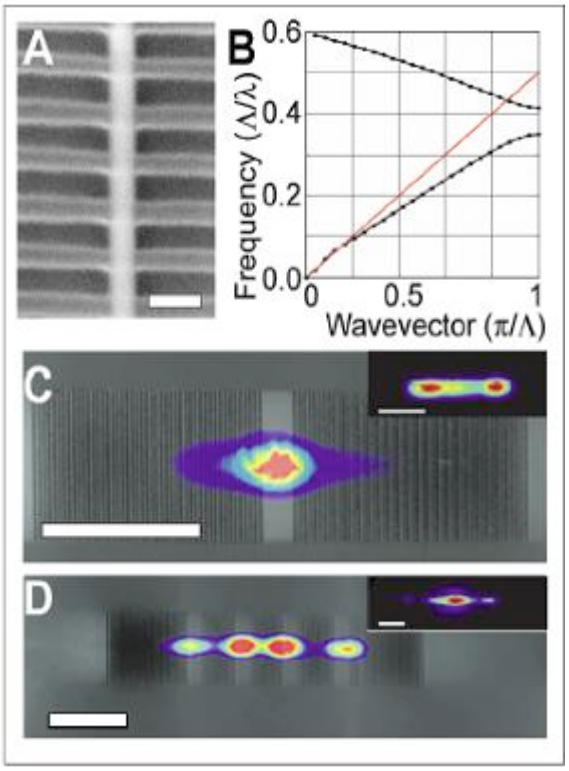

Figure 6.19. Evidence of light inhibition and localized emission in nanowire photonic crystal. **(A)** SEM image of the nanowire photonic crystal. Scale bar, 200 nm. **(B)** Dispersion diagram calculated by FDTD simulation showing the presence of a photonic band gap. Red line is the light line in air. **(C)** Photoluminescence (PL) image (false color) superimposed onto the AFM image (greyscale) of a nanowire photonic crystal with one engineered defect. Inset: Photoluminescence image of the same nanowire in absence of the photonic crystal. Scale bar, 5 μm. **(D)** PL image (false color) superimposed onto the AFM image (greyscale) of nanowire photonic crystal with four distinct engineered defects. The dotted line indicates the nanowire position. Inset: PL image of the same nanowire in absence of the photonic crystal. Scale bar, 5 μm.

In contrast to photonic crystal cavities based on distributed feedback, these nanowire racetrack microresonators trap light by total internal reflection. The optical micrograph (Figure 6.20A) shows the racetrack microresonator (2-μm-wide track) defined in PMMA and 11.2–μm-long CdS nanowire (200 nm diameter) embedded in one arm. The total optical length of the resonator, taking into account the refractive indices of PMMA and CdS, is approximately 130 μm. PL imaging shows light emitted from the nanowire waveguided by total internal reflection around the racetrack microresonator (Figure 6.20B). PL spectroscopy was carried out to investigate the spectral emission of the structure. The modes of the racetrack resonator can clearly be seen in the PL spectrum (Figure 6.20C). The periodicity of the modes in terms of inverse wavelengths is 7.9×10^{-3} μm^{-1} indicating an optical length of around 127 μm. This is in an excellent agreement with the optical length of the racetrack resonator estimated to be 130 μm. This optical length corresponds to the fundamental mode circulating around the racetrack microresonators, guided by total internal reflection, as suggest by the PL image. Finally strong evidence of optical gain (amplified spontaneous emission) is shown in Figure 6.20D.

Near-field Laser Antennas

This work, which has led to a major advance by **Capasso**'s and **Crozier**'s group, i.e., the demonstration of a new photonic devices capable of generating intense nanospots for applications such as ultrahigh density optical recording, has been described in the report of **Kenneth Crozier.**

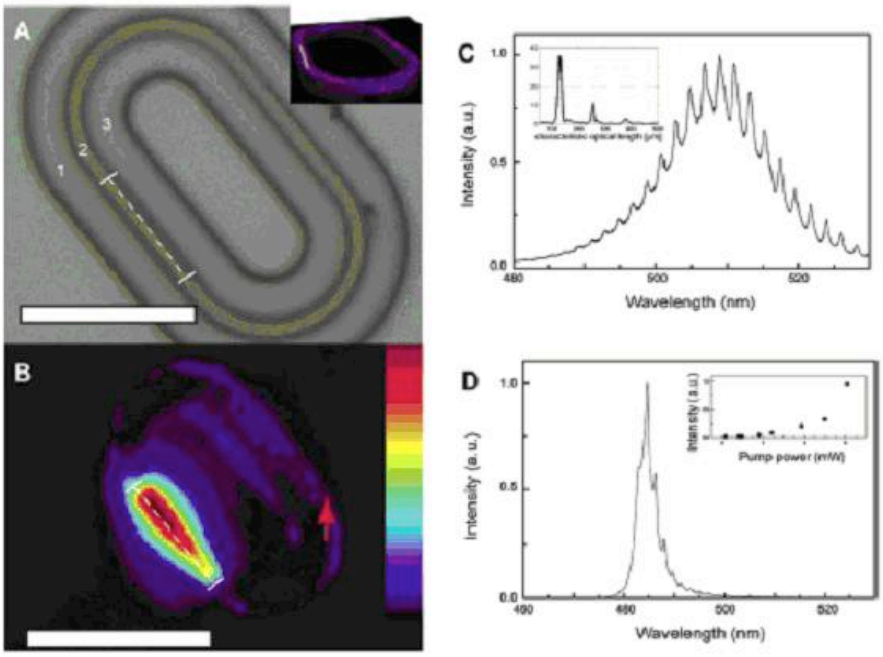

Figure 6.20. Nanowire racetrack microresonators**. (A)** Optical micrograph of nanowire racetrack microresonator. The nanowire is embedded in the left arm of the microresonator The dotted line indicates the nanowire position. **(B)** Photoluminescence image of the nanowire racetrack microresonanor. Both scale bars in **(A)** and **(B)** are 20 mm. The red arrow indicates the region over which the spectra were collected. **(C)** Racetrack cavity modes observed at room temperature in the photoluminescence spectrum. **(D)** Spectrum measured at low temperature of ~4K. Inset, superlinear increase in peak output power versus incident pump power.

Synthesis, Imaging and Electron Transport in 2-D Metal Chalcogenides

Cynthia M. Friend
Chemistry and Applied Physics, Harvard University
Collaborator: Charles Marcus (Harvard)

Recently, there has been a renewed interest in the study of electronic transport through a material consisting of a single atomic layer. The **Friend** group in collaboration with the **Marcus** group has focused on preparing well-defined 2-D materials and integrating them into devices so as to study electron transport in these materials. Our efforts have included the synthesis of 1-layer high metal dichalcogenides (TiS_2 and MoS_2) and graphene.

A novel method for growth of well-defined metal disulfide nanostructures was developed in the **Friend** lab. For example, TiS_2 nanocrystals that are one layer high are grown on Au(111) by

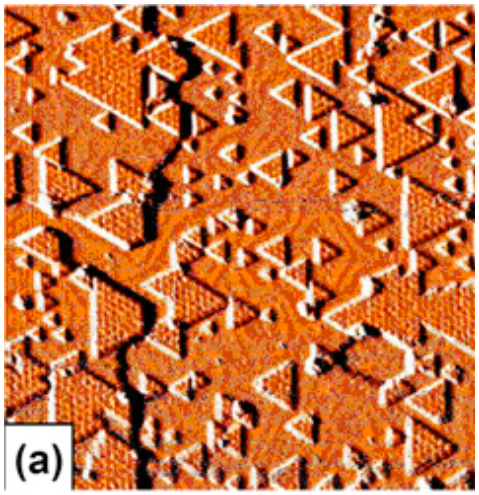

Figure 6.21. STM image of 1 atomic layer high TiS_2 nanostructures grown on a Au substrate. The image is 150 x 150 nm.

first sulfiding the Au and subsequently depositing Ti. The nanostructures crystallize upon heating to 670 K in vacuum. The Ti:S ratio can be accurately controlled using this method enabling us to create materials with specific defects. In order to further investigate electron transport in these materials, they must be integrated into a device. This is planned in future work.

More recently, we have turned our attention to studies of single-layer high graphite sheets, commonly called graphene. Due to graphene's unique band structure, studies have shown that a single layer of graphene behaves like a two-dimensional layer of Dirac mass-less fermions. We have been able to probe the nature of the Dirac fermions and

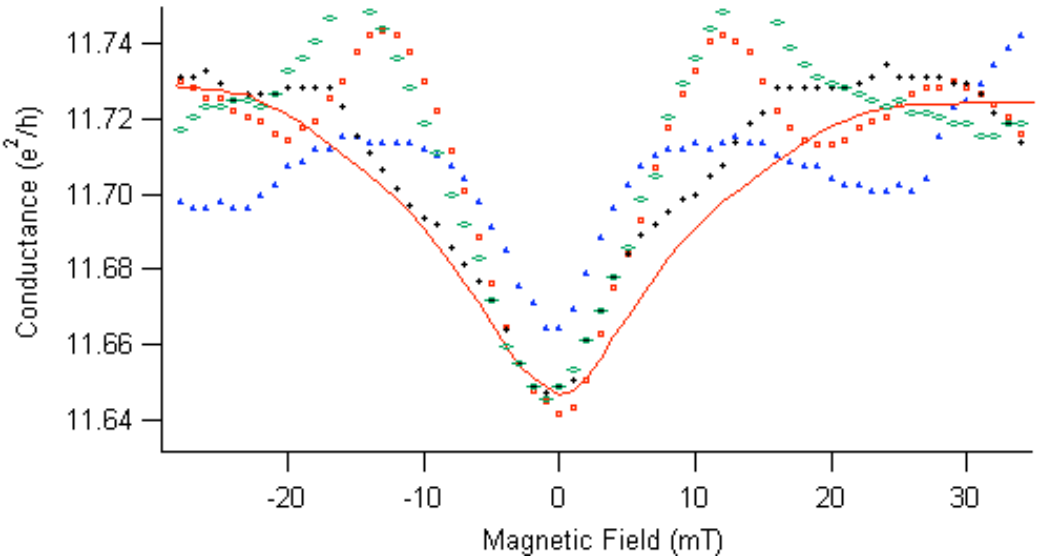

Figure 6.22. Weak localization correction to the conductivity measured for a device based on few layers of graphene.

their coherent properties through the study of quantum mechanically corrections to the conductivity. Figure 6.22 shows the weak localization correction to the conductivity. Using a novel method developed in the **Marcus** group, we have shown that pulsing the voltage on the back gate redistributes the impurity locations allowing us to generation independent members of an ensemble. Show in Figure 6.22 is average over 25 independent members of the ensemble (solid red line) along with 3 members of the ensemble (markers). This averaging technique is essential for using Random Matrix Theory to extract from the weak localization parameters important in studying the electronic transport properties of a graphene sheet. Future studies will include using this averaging technique to study in detailed weak localization at various positions in the graphene electronic band structure.

In our future work, we plan to further develop methods for growing 1-atom layer high materials, especially graphene, and to investigate the properties of these materials. Currently, we are investigating methods for percipitating a graphene sheet on SiC and for using CVD methods to growth graphene on suitable substrates, e.g., Si or SiC. We also plan to further investigate electron transport in the metal dichalcogenides

Theory of Electron and Spin Transport in Nanostructures

Bertrand I. Halperin
Physics, Harvard University
Collaborator(s): Raymond Ashoori (MIT), Charles M. Lieber, Charles M. Marcus (Harvard), Robert M. Westervelt (Harvard)
International Collaborator: Leo Kouwenhoven (Delft)

The overall goal of this work is to gain a better understanding of the electronic structure of nanoscale building blocks, and of the operations of nanoscale devices, in order to improve our ability to design and construct such devices. A crucial aspect of the development of new structures and devices are measurements to characterize these structures. Theoretical efforts are necessary to understand the results of such measurements as well as to suggest new types of measurements as well as possible improved structures. Our projects are motivated by NSEC-supported experiments including particularly measurements of transport in semiconducting nanowires, and imaging of electron flow and electronic states in structures made from two-dimensional electron systems. Goals include development of theoretical and calculational techniques, as well as applications to specific systems.

InAs nanowires are a particularly interesting system for fabrication of nanoscale semiconducting devices, and they are being actively studied in many laboratories, including the **Westervelt** and the Kouwenhoven groups, among others. We are trying to understand better the nature of the electronic states in these wires, and we are trying to see how much information one may gain by analyzing electrical transport in the presence of an applied magnetic field. Together with Junior Fellow Yaroslav Tserkovnyak, we became interested in this subject two years ago, when researchers in **Charles Lieber**'s group made measurements on several InAs nanowires, and found complex oscillatory behavior as a function of magnetic field, for fields both parallel and perpendicular to the sample. Using a simple model, we obtained results, which were qualitatively similar to the experimental results, but details were dependent on the assumptions we put in for such parameters as the mean-free path or the carriers, the nature of the contact to leads, and boundary conditions at the ends of the wires. Of particular interest to us were dependences on the nature of the electronic wave functions in the radial direction. For example, one obtains substantial differences if one assumes that the doping is primarily due to surface charges, and the electron states are confined near the surface of the InAs, or if one assumes that the electronic wave functions persist into the center of the wire. In principle, one should be able to back out information about the radial dependence of the electronic wave functions from the magnetic field dependence of the conductance, at least if the mean-free path is sufficiently large, and if one understands the other parameters of the system.

As **Charles Lieber** became more interested in other systems, the experiments in his group were not continued and we did not have sufficient data to work with. The theoretical work was put on hold, as we worked on other problems. However, there is now a renewed interest in InAs nanowires, within NSEC and elsewhere, and there is promise of extensive new magneto-transport data on these systems. Some measurements have already been carried out at Delft, and also by Samuelsen's group in Sweden. Mike

Stopa, at Harvard, is setting up to do detailed electronic structure calculations on InAs nanowires with a variety of possible surface treatments. Consequently, we have reopened our work on the theory of magnetotransport in these systems.

The work described above is focused on properties of a free-standing nanowire, where there is at least approximate rotational symmetry around the wire axis. Additional complications occur if the wire is on a substrate, or is perturbed by an asymmetric gate. Other interesting features occur if the carriers are depleted so that a section of the wire becomes insulating, or nearly so. At some point, effects of the interaction between electrons become non-trivial. Details of the junction between low-density and higher-density regions of the wire may also be important in determining transport and magneto-transport properties of a gated wire. We are working on Hartree-Fock techniques that may be useful in this situation, both near equilibrium and in the presence of finite bias.

Spin-orbit effects have been a major theme of our NSEC-supported work during the past few years. Recent developments have focused on transport in two-dimensional electron and hole systems, including the so-called spin-Hall effect. Analysis has shown a surprising subtlety in these problems, which has resulted in a number of conflicting results in the literature. Work is continuing to sort out these problems, including the effects of applied magnetic fields and the effects of various boundary conditions. Spin-orbit coupling has interesting effects on electron trajectories, which should be visible, in principle, in imaging experiments. Estimates suggest that these effects would be difficult to observe in GaAs systems, but might be visible in InAs or other materials. It is hoped that the **Westervelt** group will be able to carry out imaging experiments on such materials, so that interaction between theory and experiment will be possible.

A significant accomplishment during the period March 2005–March 2006 was the completion of a calculation of the spin Hall conductivity for a two-dimensional hole-gas in a semiconductor with small angle impurity scattering (Shytov *et al*., 2006). Although earlier calculations for the electron gas found vanishing spin Hall conductance regardless of the form of the impurity scattering, and calculations for holes with isotropic scattering had obtained a simple, universal result, we have found that for holes with angle-dependent scattering the result, surprisingly, depends on details of the model, including the form of the scattering and the deviations from parabolicity of the energy dispersion. Also, in March 2006, we completed the manuscript of a review article on spin Hall effects, to appear in the Handbook of *Magnetism and Advanced Magnetic Materials*, edited by S. Parkin and D. Awschalom (Engel *et al*., 2006).

Imaging experiments in **Ashoori**'s laboratory have revealed surprising structure in quantized Hall states, which we are trying to better understand. The general picture emerging from the data suggests that there are puddles of relatively high longitudinal conductivity embedded in a percolating network of quantized Hall regions with essentially vanishing conductivity, but that electrons can transfer from one conducting region to another by tunneling through defects, in a process that can be extremely efficient when they are tuned to a resonance. We are trying to understand more precisely the fluctuations leading to this conductivity, and the nature of the defects that cause resonant tunneling between them.

References

A. V. Shytov, E. G. Mishchenko, H.-A. Engel, and B. I. Halperin, "Small-angle impurity scattering and the spin Hall conductivity in two-dimensional semiconductor systems," *Phys. Rev. B* **73**, 075316 (2006).

H.-A. Engel, E. I. Rashba, and B. I. Halperin, "Theory of spin Hall effects," to appear in the *Handbook of Magnetism and Advanced Magnetic Materials*, edited by S. Parkin and D. Awschalom. (*cond-mat*/0603306) (2006).

Snapshot of DNA Translocation Through a Nanopore

Efthimios Kaxiras
Physics and Applied Physics, Harvard University
Collaborator: George M. Whitesides (Harvard)

We applied a theoretical multiscale methodology for the study of biological processes such as the translocation of biopolymers through membrane pores. These kinds of phenomena play a major role in many phenomena, such as viral injection by phages, gene therapy, etc. From a technological point of view, recent experimental work has focused on the possibility of fast DNA-sequencing upon 'reading-off' the DNA sequence by tracking its motion through nanopores. In these experiments the molecule is moving in the presence of a fluid solvent under the influence of an electric field applied at the pore region. Therefore, in order to simulate such complex systems there is a need to model the behavior simultaneously at several length and time scales.

More specifically, we simulate the biomolecule dynamics using a multiscale methodology for dealing with the continuum as well as the molecular scales in a complex fluid. The methodology is based on a combination of the Lattice Boltzmann Equation for handling fluid flow at the continuum scale, and Molecular Dynamics simulations for handling the molecular scale. A unique feature of the present approach is that hydrodynamic interactions between the solute biomolecules and the aqueous solvent are treated explicitly, and yet in a computationally efficient way. This methodology can be applied to issues of microfluidics and the interaction of biological macromolecules with cell membranes.

Using the above approach we studied the translocation of DNA through a nanometer pore. A force is applied at the hole region that pulls the molecule through the hole. We performed a series of simulations for different initial realizations of the DNA structure and various lengths. From this the duration histograms were constructed and the most probable translocation time for each length was calculated, leading to a power-law dependence of this time on the molecule length. Hydrodynamic coherence was evident in all our calculations, since the fluid imposes random fluctuations to the DNA motion.

The theoretical tools we have developed are appropriate for microfluidic and related applications such as the interaction of biological macromolecules with cell membranes and the vesicle wall. These problems are relevant to experimental work of the **Whitesides**' and **Mizgerd**' groups in Cluster 1. Interactions with these groups will be

pursued, once the methodologies have been thoroughly tested on model system, like the DNA translocation through a nanopore discussed above.

Photonic Systems

Charles M. Lieber
Chemistry and Applied Physics, Harvard
Collaborators: Federico Capasso, Robert M. Westervelt (Harvard)

Lieber and coworkers have developed a hybrid approach for photonic systems that combines chemically-synthesized single nanowire emitters with lithographically-defined photonic crystal and racetrack microresonator structures. Finite-difference time-domain calculations were used to design nanowire photonic crystal structures where the photonic band gap overlaps the electronic band gap of the nanowire. Photoluminescence (PL) images of cadmium sulfide (CdS) nanowire photonic crystal structures designed in this way demonstrate localized emission from engineered defects and light suppression in regions of the photonic crystal. PL spectroscopy studies of defect-free nanowire photonic crystal structures further demonstrate the photonic band gap or stop band that spans most of the CdS band edge emission spectrum. In addition, single CdS nanowire-racetrack microresonator structures were fabricated, and PL imaging and spectroscopy measurements show good coupling of the nanowire to the microcavity including efficient feedback and amplified spontaneous emission. These hybrid structures exploit unique strengths of bottom-up and top-down approaches and thereby open new opportunities in nanophotonics from efficient and localized light sources to integrated optical processing.

Electronic Noise in Nanoscale Devices

Charles M. Marcus
Physics, Harvard University
Collaborators: Cynthia M. Friend, Bertrand I. Halperin (Harvard)

Several accomplishments in the subject of **electronic noise in nanoscale devices** from the **Marcus** group were supported by NSEC funding. Among those accomplishments were the following two highlights: (1) realization of a two-channel system for measuring auto- and cross-correlation of current noise at low temperatures (submitted to *Review of Scientific Instruments*) and (2) measurement of shot noise in a quantum point contact in a magnetic field, revealing signatures of the 0.7 structure and spin (submitted to *Physical Review Letters*). These are briefly described below, in order.

A Two-Channel Noise Detection System

Our Noise Team (including two graduate students and one undergraduate) has designed and implemented a practical system for measuring the current noise (temporal

fluctuations) in multi-terminal mesoscopic devices operating at cryogenic temperatures. This system, employing low-noise cryogenic amplification and real-time signal processing, can measure the power and cross-spectral density at MHz frequencies of the shot noise in two sub-nanoamp currents.

The temporal fluctuations of the electronic currents in mesoscopic conductors are sensitive to quantum statistics, scattering and many-body effects, and can manifest effects not evident in dc (time averaged) transport. The demonstrated performance of this system puts us in a unique position to perform noise-based investigations of mesoscopic transport with a focus on electron-electron interactions (Coulomb charging, dephasing, and inelastic scattering) and two-particle interference (exchange).

Shot-Noise of a Quantum Point Contact in a Magnetic Field

In the first study using the noise detection system, we measured the shot noise of a GaAs quantum point contact in the presence of an in-plane magnetic field. As shown in Figure 6.23, we observe at zero field an asymmetry in shot noise associated with the 0.7 structure in conductance. The underlying microscopic origin of the 0.7 structure, believed to be a many-body spin effect, remains an open problem in mesoscopic physics. The asymmetry in noise evolves smoothly into the symmetric signature of spin-resolved electron transmission at high field. We find quantitative agreement between experiment and a phenomenological model for a density-dependent level splitting.

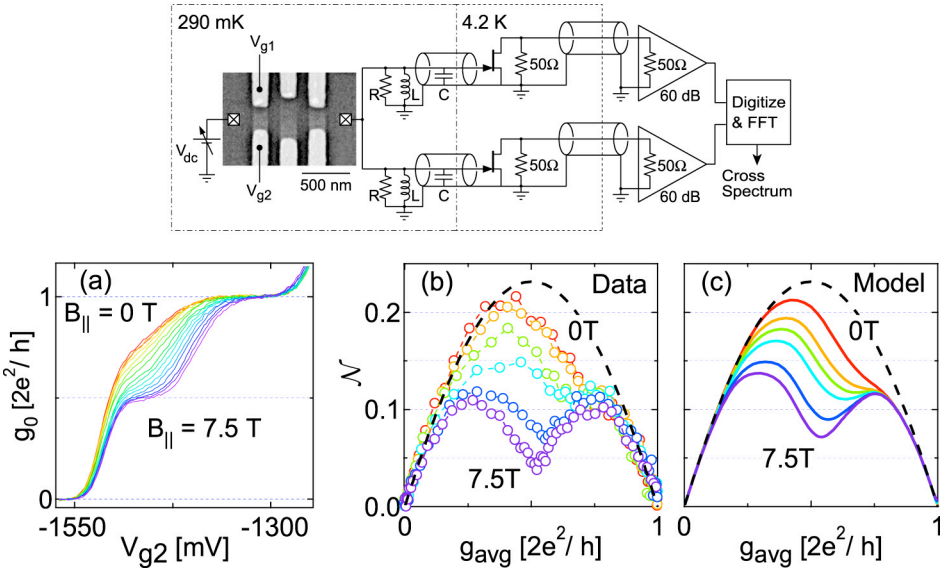

Figure 6.23. Equivalent circuit at 2 MHz of the two-channel system measuring shot noise of a quantum point contact as a function of in-plane magnetic field, including an electron micrograph of the GaAs device. Measured linear conductance in (a) shows a shoulder-like 0.7 structure at zero field. The structure evolves smoothly into the 1/2 x 2 e^2/h spin-resolved plateau at high field. Noise data in **(b)** show an asymmetric dome at zero field, with a reduction in noise associated with the 0.7 structure in conductance. The dome evolves smoothly into a symmetric double-dome at high field, which is the signature of spin-resolved transmission. A phenomenological model for a density-dependent level splitting **(c)** shows quantitative agreement with noise data, with model parameters extracted solely from conductance. From "Shot-Noise Signatures of 0.7 Structure and Spin in a Quantum Point Contact" by L. DiCarlo*, Y. Zhang*, D. T. McClure*, D. J. Reilly, C. M. Marcus, L. N. Pfeiffer, K. West, cond-mat/0604019 (2006) (submitted to *Phys. Rev. Lett.*). *Noise Team members (including one undergraduate) contributed equally to this work.

Synthesis and Characterization of Single-Crystalline e-FeSi Nanowires

Hongkun Park
Chemistry, Harvard University
***Collaborator*:** Charles M. Lieber (Harvard)

In the grant period 2005–2006, we have synthesized single-crystalline ε-FeSi nanowires and characterized their electrical and magnetic behaviors by wiring them up individually. As shown in the scanning electron microscopy (SEM) image in Figure 6.24a, the synthesis yields single-stem wires and branched wires with triangular 'thorns' on their stems. Typical radii of these nanowires range from 5 nm to about 100 nm, and their lengths vary from a few hundred nanometers to tens of micrometers. A representative transmission electron microscope (TEM) image in Figure 6.24b shows that these nanowires exhibit a cubic ε-FeSi structure just as in their bulk counterpart and that the nanowire growth is along the [111] direction. Notably, the diffraction pattern did not change as the electron beam was moved along the nanowire, indicating that the whole nanowire is a single crystal.

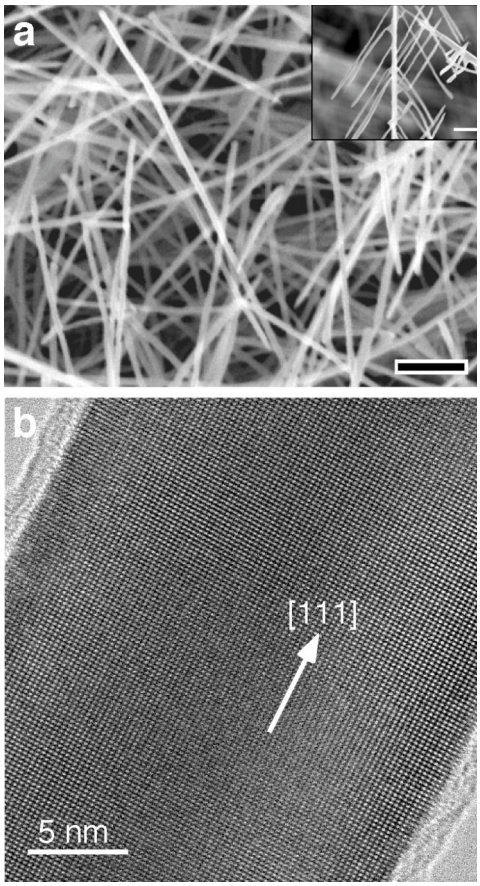

Figure 6.24. (a) SEM image of ε-FeSi nanowires as grown on a silicon substrate. Inset: SEM image of a nanowire with both branches and triangular 'thorns'. Both scale bars represent 500 nm. **(b)** High-resolution TEM image of a FeSi nanowire with growth direction parallel to the [111] direction.

The electrical conductivity of individual FeSi nanowires was measured as a function of T by contacting them in a four-probe geometry using electron-beam lithography and thermally evaporated Cr-Au electrodes (Figure 6.25a, inset). Two different types of transport were observed in these samples. The first type, exhibited by single-stem nanowires without branches, is shown in Figure 6.25a. Here the nanowire resistivity, ρ, falls over an order of magnitude when T is raised from 2 to 20 K. Following a plateau between 20 and 50 K, the resistivity drops steeply again, approaching a saturation value of $\sim 2 \times 10^3$ μΩ cm at room temperature. This thermally activated behavior is similar to that observed in bulk FeSi: the drop in ρ below 20 K is attributed to the excitation of states within the band gap, while the drop above 50 K reflects the increase in charge-carrier concentration, n_c, due to carrier excitation over the band gap. Making the assumption that $n_c \propto 1/\rho$, the gap energy, E_g, can be extracted from the slope of $\ln(1/\rho)$ versus $1/k_BT$ using the thermal activation equation: $\ln(n_c) \propto \ln(1/\rho) \propto -E_g/(2k_BT)$. From a fit to the data in Figure 6.25a between 93 and 193 K, E_g is found to be 50 meV, at the lower end of the range of E_g values reported for bulk FeSi.

The second type of transport behavior, exhibited primarily by nanowires with branches or thorns, is shown in Figure 6.25b. Here the resistivity rises between 5 and 50 K, followed by a fall to ~ 400 μΩ cm at room temperature. The rise in ρ below 50 K is typical of a metal, while the fall at higher T is consistent with the thermal activation behavior discussed above, with a band gap of $E_g \approx 44$ meV. This crossover between metallic and semiconducting behavior is consistent with a heavily doped narrow band-gap model, and suggests that branch-induced charge-carrier introduction may play a substantial role for branched FeSi nanowires. In this scenario, the Fermi energy lies within a conduction or a valence band in branched FeSi nanowires, and the transport is determined by a competition between the carrier scattering and the thermal excitation of carriers over the band gap. At low T, where $\partial\rho/\partial T$ is positive, thermal energy is insufficient to change the charge-carrier concentration appreciably, and the increase in carrier scattering with T dominates. Above 50 K, excitation of carriers over the band gap becomes significant, thereby lowering ρ. The fact that branched nanowires show metallic behavior at low temperatures suggests that that junctions between the stem and branches may act as a source of charge carriers, either by deviation from the ideal stoichiometry or by the introduction of lattice defects.

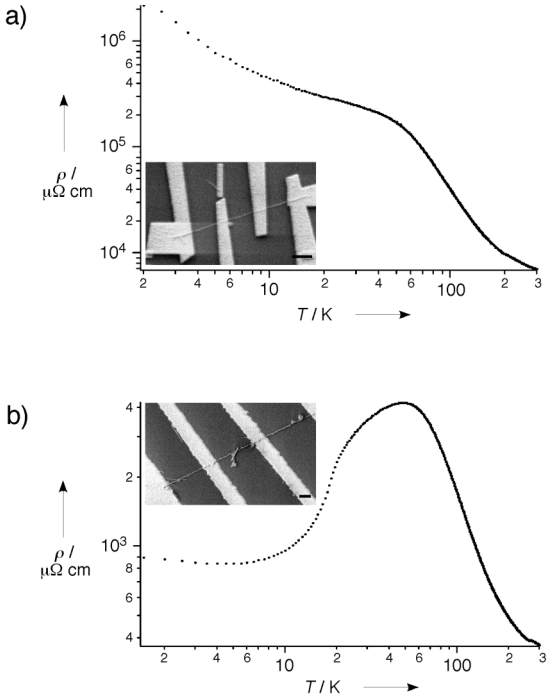

Figure 6.25. (a) A plot of ρ as a function of T obtained from a representative single-stem nanowire. Here the nanowire diameter is 40 nm and the length between electrodes is 1.4 μm. Inset: SEM image of the nanowire device. **(b)** A plot of ρ as a function of T obtained from a representative branched nanowire. The nanowire diameter is 45 nm and the length between electrodes is 3.8 μm. Inset: SEM image of the nanowire device. In **(a)** and **(b)**, the scale bar in the inset is 1 μm.

CLUSTER 3: Imaging Electrons at the Nanoscale

Coordinator: Raymond Ashoori

Raymond Ashoori (Physics, MIT)
Kenneth Crozier (DEAS, Harvard)
Arthur Gossard (Materials, UCSB)
Eric Heller (Chemistry & Physics, Harvard)
Jennifer Hoffman (Physics, Harvard)
Marc Kastner (Physics, MIT)
Venky Narayanamurti (DEAS & Physics, Harvard)
Pierre Petroff (Materials, UC Santa Barbara)
Robert Westervelt (DEAS & Physics, Harvard)

***Collaborators*:** Michael Stopa (NNIN, Harvard)

International Collaborators: Fabio Beltram (NEST, Pisa, Italy), Leo Kouwenhoven (TU Delft, The Netherlands), Daniel Loss (University of Basel, Switzerland), Hiroyuki Sakaki (University of Tokyo, Japan), Seigo Tarucha (University of Tokyo and NTT, Japan)

Number of postdoctoral fellows: 2
Number of graduate students: 6
Number of undergraduate students: 5

Introduction

Electrons inside nanoscale structures display striking quantum behavior that arises from the confinement of electron waves. By visualizing how electron charges and spins move through nanoscale systems, we can understand the fundamental science and develop new quantum devices. These devices can control a single electron charge or spin to form, to develop a quantum switch for future ultrasmall electronics, or to implement qubits for quantum information processing.

Nanoscale structures also offer new opportunities for photonics. New custom-made tips for Near-field Scanning Optical Microscopy (NSOM) can be used to image an perturb photonic systems, and nanowires can be made into electro-optical devices.

The goal of this Cluster is to develop new ways to image the quantum behavior of electrons and photons in nanoscale systems. This is difficult for electrons, because they are buried inside the structure, and because low temperatures are necessary. Imaging photons at the nanoscale requires new approaches and new electro-optic devices. Custom-made microscopes and new imaging techniques are needed. This Cluster brings together participants who are known for their skill in designing custom-made scanning probe microscopes (SPMs) and in developing new ways to image the quantum effects inside nanoscale systems. A close collaboration with the MBE Lab at UC Santa Barbara to make custom-designed heterostructures makes this work possible. The Cluster has strong international collaborations with Fabio Beltram (NEST), Leo Kouwenhoven (TU Delft), Daniel Loss (Univ. Basel), Seigo Tarucha (U Tokyo & NTT) and Hiroyuki Sakaki (U Tokyo).

Expected outcomes of this research are:

New Approaches in Scanning Probe Microscopy for Imaging the Quantum Behavior of Nanoscale Systems — Custom-made microscopes with new imaging techniques, coupled with theoretical simulations, will allow us to understand the quantum

behavior of electrons and photons in nanoscale systems. The approaches include microscopy with liquid cooled Scanned Tunneling Microscopes (STMs) and cooled Scanning Probe Microscopes (SPMs), Ballistic Electron Emission Microscopy (BEEM) and Ballistic Electron Emission Luminescence (BEEL) Microscopy, and Near-field Scanning Optical Microscopy (NSOM) with custom tips. Knowledge of the quantum behavior will allow us to make and test new nanoscale electronic and photonic devices and systems.

New Nanoscale Electronic and Photonic Devices — By using scanning probe microscopes as tools we can learn how to control electrons and photons in new types of electronic and photonic devices. Advances in MBE growth at UC Santa Barbara can form self-assembled InAs quantum dots that can be used to make new electronic and photonic devices. Nanowires and nanoparticles synthesized from new materials in Cluster 2 offer exciting opportunities for electronic and optical devices. Imaging electrons and photons in these structures will allow us to make and understand these new devices.

Major Accomplishments

Two new faculty members at Harvard have been added to our Center in its renewal: **Jennifer Hoffman** and **Kenneth Crozier**. Both are building new scanning probe microscope systems in their research labs.

Jenny Hoffman is making a sophisticated UHV STM that can be cooled to liquid He temperatures, she has experience using and building systems of this type by working in Seamus Davis's lab at Berkeley as a grad student. This instrument will allow the study of quantum effects on clean surfaces with atomic resolution.

Kenneth Crozier is developing custom-made NSOM tips that have a conical form, with a microlens on top. Unlike conventional drawn fiber tips, these are robust, with high optical throughput. **Ken Crozier** plans to add a small metal antenna to focus the electromagnetic field at the pointed end of the tip for subwavelength imaging. Scanning probe imaging of an optical antenna fabricated on the end of a semiconductor laser chip, show the concept works very well.

Frontiers in Nanoscale Science and Technology Workshop. Our third international workshop was held on January 26–28, 2006 in San Francisco. The workshop brought together international collaborators of the Center including Daniel Loss, Lars Samuelson, and Seigo Tarucha, and other outstanding researchers from Japan and Europe. The first day was devoted to industrial, and the development of ultrasmall quantum switches for the Nanoelectronics Research Initiative. Three representatives from the electronics industry presented talks: Pushkar Apte (SIA), Robert Doering (TI), and George Bourianoff (Intel). They were joined by talks on oxide switches and nanowire electronics. Imaging and quantum information processing were addressed in the following two days.

Subsurface Charge Accumulation Imaging of the 2-D Electron Gas

Raymond Ashoori
Physics, Massachusetts Institute of Technology
Collaborators: Bertrand I. Halperin, Pierre Petroff (UCSB)

We have developed a means of imaging charge transport on small length scales in the quantum Hall effect using a scanning charge accumulation microscope (Steele *et al*., 2005). Applying a DC bias voltage to the tip induces a highly resistive ring-shaped incompressible strip (IS) in a very high mobility 2-D electron system (2DES). The IS moves with the tip as it is scanned, and acts as a barrier that prevents charging of the region under the tip. At certain tip positions, short-range disorder in the 2DES creates a quantum dot island inside the IS that enables breaching of the IS barrier by means of resonant tunneling through the island. Striking ring shapes appear in the images that directly reflect the shape of the IS created in the 2DES by the tip. Our simulations show that native disorder from remote ionized donors can create the islands, and comparison of the images with simulations provides a direct and quantitative view of the disorder potential of a very high mobility 2DES.

Through our measurements of leakage across the IS, we extract information about energy gaps in the quantum Hall system. Varying the magnetic field, the tunnel resistance of the IS varies significantly, and takes on drastically different values at different filling factors. Measuring this tunnel resistance provides a unique *microscopic* probe of the exchange-enhanced spin gap, and potentially of other quasi-particle gaps in quantum Hall systems. We also draw a connection to bulk transport. At quantum Hall plateaus, electrons in the bulk are localized by a network of ISs. We have observed that the conductance across one IS is drastically enhanced by resonant tunneling through quantum dot islands. Similarly, this resonant tunneling process may play a pivotal role in dissipative transport at quantum Hall plateaus.

We have developed simulations of the interaction of a metallic scanning probe with a 2-D electron system (2DES) in the quantum Hall regime. The simulation is based on an electrostatic relaxation method, modified to include the nonlinear screening of the 2-D electron system at high magnetic fields. Using 2-D simulations with cylindrical symmetry that allow us to account for the exact shape of the tip, we predict the diameter and width of ring shaped incompressible strips (ISs) induced by DC tip biases. Extending these results to 3 dimensions, we incorporate the effect of the disorder on the shape of the IS, and predict the formation of quantum dot islands observed in Steele *et al*. (2005). Comparison of the simulation results with experimental data provides a direct and quantitative view of the disorder of a very high mobility 2DES. Michael Stopa of the NNIN provided useful advice in developing the simulations.

We are now working to further characterize quantum dot islands in the incompressible strip and searching for unusual many body transport (such as singlet-triplet Kondo effect that can occur in a high magnetic field) through these objects. Ultimately, this experiment examines transport on the smallest length scales and has led us to discover previously unpredicted small-scale structures (quantum dots) within this heavily studied system.

G.A. Steele, R.C. Ashoori, L.N. Pfeiffer, and K.W. West, *Phys. Rev. Lett.* **95**, 136804 (2005).

InAs Self-Assembled Dots

We are initiating a project with NSEC member **Pierre Petroff** to perform capacitance spectroscopy on single InAs self-assembled quantum dots. These self-assembled quantum dots have potential applications ranging from single-photon sources for quantum computing, quantum dot lasers, and as floating gate structures for extremely small and reliable flash memories. All prior capacitance measurements in this system have been performed in arrays of quantum dots and have not yielded sufficient spectral resolution to ascertain much of the underlying physics of the dots. Measurement on a single dot will allow determination of the effects of electron-electron interactions and eventual comparison of optical spectra on a single dot. Also, we will be able to study charging in small clusters of dots to observe the effects of Coulomb interactions between dots on the charging spectra. We may eventually learn to control charging in multiple dots that are connected by barriers controllable through gating.

This collaboration represents a merger of world-class molecular beam epitaxial techniques from a pioneer of InAs quantum dot research with single-electron capacitance measurements that are unique to the **Ashoori** lab. No other groups have demonstrated the capability of performing capacitance spectroscopy with single electrons in semiconductor quantum dots.

Capacitance Imaging of 2-D Hole Systems

2-D hole systems in GaAs have been proposed as a foundation for spintronic devices. The strong spin-orbit interaction allows the possibility for creating devices using the Rashba Effect to preferentially control one spin state. We aim to examine this system, on the microscopic level, in a similar fashion to what we have done with electrons. We can determine the character of the self-consistent electrostatic potential within this system. Moreover, we will examine a system with density that can be varied through the 2-D metal-insulator transition. There is even the possibility of direct observation of Wigner crystallization in this system at low temperatures. The samples are obtained in collaboration with M. Manfra, L. Pfeiffer, and K.W. West, all of Bell Labs, Lucent Technologies. Theory support for this work will come from **Eric Heller** and **Bertrand Halperin**.

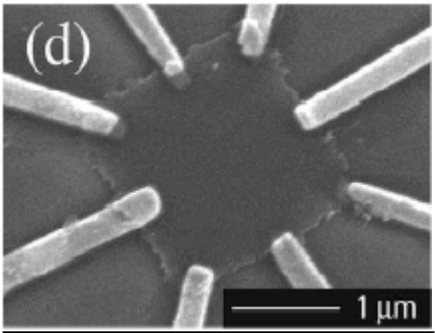

Figure 6.27. Picture of a Hall bar created from a graphene sheet. From a paper from Philip Kim's lab at Columbia.

Physics of Graphene Sheets

Andre Geim's lab at the University of Manchester in the UK recently announced a fantastic discovery. They found that by simply rubbing graphite on surfaces (and later applying ultrasound to the surfaces to flake off excess graphite) they can deposit isolated monolayers of graphite (graphene sheets). Extraordinarily, they found it was easy to make electrical contacts and

to fashion Hall bars from the material. At low temperatures, the graphene sheets actually display the quantum Hall effect! This effect has been reproduced in Philip Kim's lab at Columbia, and they have found mobilities as high as 15,000 cm^2/Vs. The physics of the QHE in these structures is quite different from other 2-D systems. Other than the valley degeneracy, the band structure has a linear rather than parabolic dispersion relation, and although Landau level structure exists (the levels are no longer evenly spaced in energy), the derivation involves solving a Dirac equation. Another feature of the material is that it can easily be field-effect-doped with a back gate with electrons or holes.

Obviously, this new technology is very interesting for a number of technological reasons. Carbon appears to have an amazing immunity to developing surface traps that drastically lower the mobility of most field effect devices. Indeed, it took many years to develop CMOS transistors, and the main difficulty was overcoming the threshold broadening induced by surface states. Carbon nanotubes transistors, on the other hand, simply worked, essentially on the first try. The carbon nanotubes have also displayed very high current carrying capacities and high transconductances. It is likely that the graphene sheets will display the same characteristics.

An obvious experiment for us is to perform our charge accumulation imaging on the graphene sheets. As the tip can, in this case be moved up directly against the surface, we can expect much higher resolution. Moreover, we will be able to perform direct STM imaging along with our capacitance techniques. We note though that capacitance has an important feature lacking in STM. In STM, the bias set between the tip and the sample controls the tunneling current and cannot be adjusted independently of the tunneling current. Therefore, even at small biases one often ends up with large electric fields between the tip and the sample due to workfunction differences. In capacitance, there is no tunneling current, and we can adjust (and null) at will the electric field between the tip and sample and thereby control the perturbation created by the tip. Finally, having the tip so close to the sample will allow for very high resolution scanned gate measurements.

We plan to perform the same types of scanning bubble experiments on graphene in the quantum Hall effect regime as we have done in GaAs. This will give us a good idea of the types of short-range disorder that exist in these structures. Later experiments may examine high current saturation in the material (as occurs in nanotubes) and conducting pathways. This is perhaps the most exciting new electronic materials systems to arise in the last decade. Knowledge both of the underlying physics and techniques for producing graphene gained in this project will have impact on the NSEC further in the future. This work will impact on our understanding of nanotubes and 2-D systems and connect with the work of **Hongkun Park** and also **Bert Halperin**.

Near-field Laser Antenna

Kenneth B. Crozier
Electrical Engineering, Harvard
Collaborator: Federico Capasso (Harvard)

Research Goal

The objective of this research is to experimentally realize an integrated photonic device that generates intense optical fields confined to subwavelength dimensions. The target applications are ultra-high density optical data storage and new sources for scanning near-field optical microscopy.

Progress/Accomplishments

Summary. We have modeled and implemented optical antennas on the facet of a commercial near-infrared diode laser, and have directly observed the highly localized enhancement of the laser field using an apertureless scanning near-field optical microscope (SNOM).

Detailed Description. A compact source with sub-wavelength spatial resolution provides distinct advantages in a number of applications (microscopy, spectroscopy, optical data storage, lithography and laser processing). Limitations on throughput of near-field scanning optical microscopy (NSOM) fibers have led to work on very-small aperture lasers (VSAL), where a sub-wavelength aperture is placed on the facet of a diode laser (Partovi *et al.,* 1999). More advanced structures, such as the C-aperture, have also been fabricated on a laser and investigated, showing improved transmission and field confinement down to 90 nm × 70 nm (Chen *et al*., 2003). In recent years, considerable attention has been given to optical antennas, in particular due to their ability to couple light very efficiently to sub-wavelength dimensions (Crozier *et al*., 2003; Schuck *et al*., 2005; Muhlschlegel *et al*., 2005).

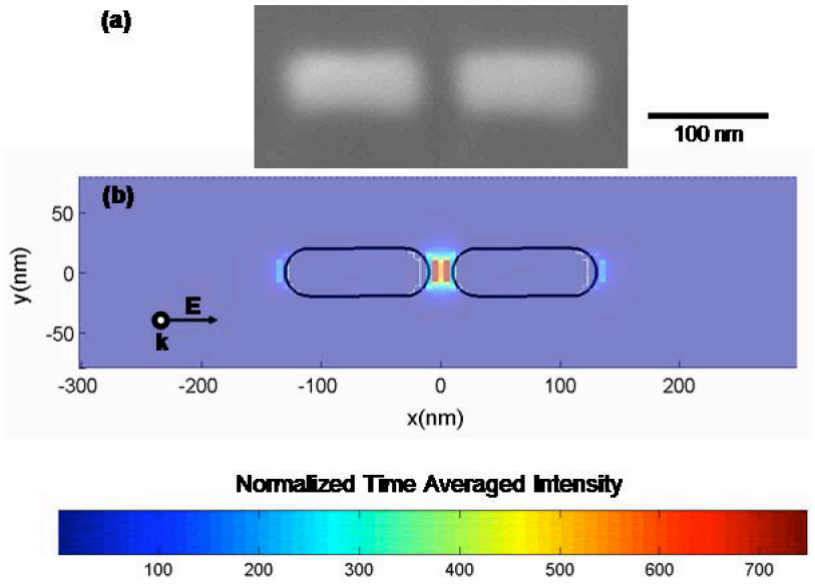

Figure 3.2. (a) Scanning electron microscope image of the fabricated structure. **(b)** FDTD simulation of electric field intensity ($<|E|^2>$) distribution on optical antenna, normalized to electric field intensity of illuminating plane wave. Electric field (E) and propagation vector (k) of illuminating plane wave are shown.

In this work we implement optical antennas on the facet of a laser, thereby creating a new plasmonic device, termed an active optical antenna. The optical antenna structure is fabricated on a commercial edge-emitting laser diode operating at a wavelength of 830 nm. To prevent electrical shorting of both the laser and the monitor photodiode of this commercial laser diode, Al_2O_3 was deposited first onto the facet as an insulating layer. A 100-nm thick Au layer was then evaporated onto the Al_2O_3 film. The nanoscale optical antenna was fabricated by focused ion beam milling (Figure 6.28 (a)). We first performed finite difference time domain (FDTD) method simulations of the antenna structures. Our optical antenna consists of two gold rectangular sections separated by a gap of 20 nm. The rectangular gold sections are 120-nm long, 50-nm wide and 50-nm thick. The ends of the rectangles are realistically rounded, with radii of curvature of 25-nm. In our simulations the incident field is polarized along the *x* direction. The time averaged electric field intensity (<|E|2>) distribution for this polarization right above the antenna structure is shown in Figure 6.28(b). The time-averaged intensity in the gap is enhanced by a factor of 700 relative to the incident intensity. Physically this enhancement is due to the charges accumulating on both sides of the gap thus generating an intense electric field in the near field zone.

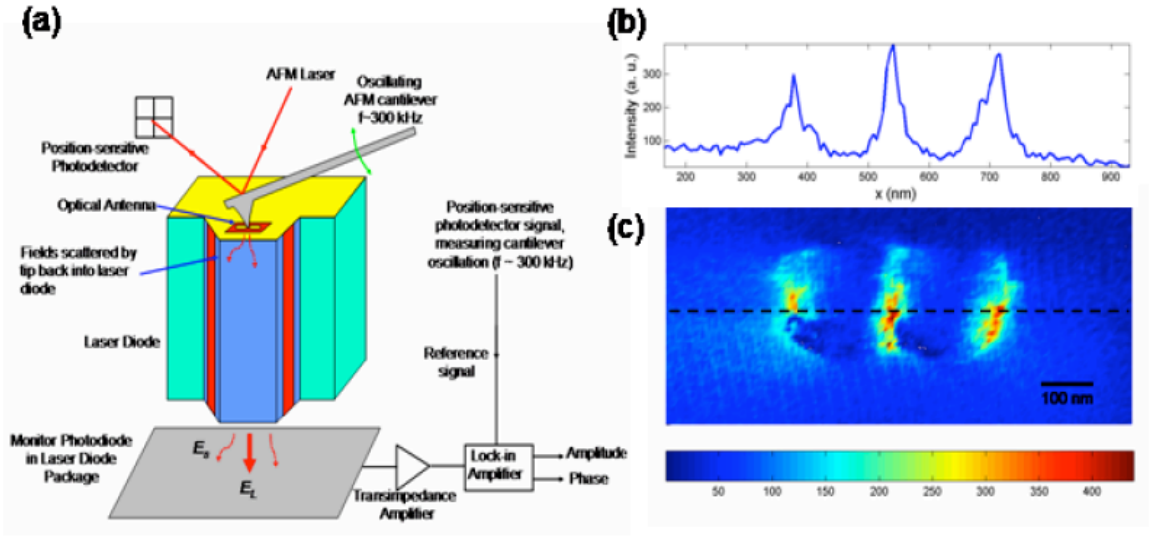

Figure 6.29. (a) Measurement of field distribution on optical antenna with scattering-type apertureless scanning near-field optical microscope. E_L – optical field on photodiode from laser diode output. E_S – optical field on photodiode resulting from sharp AFM tip scattering fields on surface of optical antenna. **(b)** Intensity distribution along the dashed line in Figure 6.29**(c)**. **(c)** Measured optical near-field intensity distribution of the antenna structure with 2 *f* detection. Color scale is in arbitrary units.

To measure these enhanced, primarily non-propagating fields we performed near field optical measurements. It has been shown that apertureless NSOM can be used to study the optical near-field of an aperture fabricated on a laser diode (Chen *et al*., 2003). The schematic of our experiment is shown in Figure 6.29(a). The laser diode is driven by a constant current source. The gold-coated silicon atomic force microscope (AFM) tip is scanned over the optical antenna in non-contact mode, with the very end of the tip

scattering light from the field distribution on the surface of the optical antenna. In general, light is scattered by the AFM tip in all directions. Some of the light is scattered back into the laser cavity and onto the monitor photodiode that collects light from the back facet of the laser diode. Note that the monitor photodiode only collects light from the back facet, since other parts of the photodiode were coated with gold during antenna fabrication. The photodetector current is pre-amplified and lock-in measurements are carried out at 1 × and 2 × the oscillation frequency of the AFM cantilever. The measured optical near-field distribution of the antenna structure with 2 *f* detection is shown in Figure 6.29(b) and 6.29(c). The size of the spot in the gap is about 30 nm in the *x* direction. Although both our antenna structure and the C-aperture (Chen *et al.,* 2003) give comparable spot sizes, the antenna structure can confine higher optical near-field intensities due to the capacitor like nature of the gap. As predicted by our simulations, we also observed intensity enhancement on the opposite ends of the structure.

Summary. We have experimentally demonstrated, for the first time, that active optical antennas produce intense and spatially confined optical fields. This compact device could lead to wide ranging applications such as optical recording, new microscopes for high-resolution spatially resolved imaging and spectroscopy, new probes for biology, laser assisted processing and repair of devices, circuits and masks and new optical tweezers.

Applications. We have identified optical data storage as an immediate application of this new technology. We are therefore partnering with a local company, TIAX LLC, in order to commercialize this technology.

References:

A. Partovi, D. Peale, M. Wuttig, C.A. Murra, G. Zydzik, L. Hopkins, K. Baldwin, W.S. Hobson, J. Wynn, J. Lopata, L. Dhar, R. Chichester, and J. H-J. Yeh, "High-power laser light source for near-field optics and its application to high-density optical data storage," *Appl. Phys. Lett.* **75**, 1515 (1999).

F. Chen, A. Itagi, J.A. Bain, D.D. Stancil, T.E. Schlesinger, L. Stebounova, G.C. Walker, and B.B. Akhremitchev, "Imaging of optical field confinement in ridge waveguides fabricated on very-small-aperture laser," *Appl. Phys. Lett.* **83**, 3245 (2003).

K.B. Crozier, A. Sundaramurthy, G.S. Kino, and C.F. Quate, "Optical antennas: Resonators for local field enhancement," J. *Appl. Phys*. **94**, 4632 (2003).

P.J. Schuck, D.P. Fromm, A. Sundaramurthy, G.S. Kino, and W.E. Moerner, "Improving the mismatch between light and nanoscale objects with gold bowtie nanoantennas," *Phys. Rev. Lett.* **94**, 017402 (2005).

P. Muhlschlegel, H.-J. Eisler, O.J.F. Martin, B. Hecht, and D.W. Pohl, "Resonant optical antennas," *Science* **308**, 1607 (2005).

Nanostructure Molecular Beam Epitaxy

Arthur Gossard
Materials Science, University of California, Santa Barbara
***Collaborators**:* Marc Kastner, Charles M. Marcus, Robert M. Westervelt (Harvard)

We have provided new MBE-grown heterostructures to both **Charles Marcus**'s group at Harvard and **Marc Kastner**'s group at M.I.T. in the past year. Last spring an AlGaAs/GaAs heterostructure delta doped with silicon to form a two dimensional electron gas (2DEG) was grown at UCSB's molecular beam epitaxy facility. The wafer was then sent to **Charles Marcus**'s group for fabrication into lithographically defined quantum dots. Recently two more samples were grown. The purpose was to attempt gain understanding into the "switching" behavior that plagues quantum dots on certain AlGaAs/GaAs wafers. This "switching," in which fluctuations in the sample cause a random change in the potential of the quantum dot, does not seem to depend on any other measurable quantity of the 2DEG. In fact very high mobility, and therefore high purity, 2DEGs have been found to make extremely poor quantum dots due to these potential fluctuations. Speculating that the origin of this behavior may be a result of the Fermi level with respect to the shallow dopant impurities within the AlGaAs layer, two Si doped AlGaAs/GaAs 2DEG structures were grow on the same day: (1) a reference 2DEG structure similar to the one grown last year (2) a second 2DEG structure that was the same as the reference except that part of the AlGaAs layer was doped with Er. Since Er is a deep state in AlGaAs, it is expected that the Fermi level will be pulled down, fully ionizing the dopants. This would make them less likely to change their charge state during the experiment.

Imaging Nanoscale Systems

Eric Heller
Chemistry and Physics, Harvard University
Collaborators: Robert M. Westervelt, Charles M. Marcus, Michael Stopa (Harvard)

Imaging nanoscale systems has become a major effort in many laboratories. It represents a paradigm shift away from ensemble averages and momentum space, into individual devices and real space. This is a necessity, not a luxury or even a choice. It is the future.

The past five years have been extremely fruitful in terms of the success of imaging in the **Westervelt** lab; we have been fortunate to publish several feature articles and covers of journals of our combined experiment/theory imaging collaborations. New science emerged, including the physics of probe backscattering in 2DEGS, the role of impurities in thermally robust fringing, and the discovery of branched flow in the electron flux paths. A new numerical technique has been invented to do thermal averaging in one shot by a quantum wavepacket technique.

The extension of many of our techniques to *spin imaging* has been initiated on the theory side by Jamie Walls of the **Heller** group. This is nontrivial and will require

considerable effort to develop the basic methods, and then to simulate experiments as they are planned or completed in order to better understand them, as we have done so successfully in the past without including spin. An example of a preliminary calculation of 2DEG electron spin polarization caused by collision with a spinful scatterer is shown here; note the "downstream" induced polarization. Note too that this work is far from finished, since this is a theorist's image and not the mock up of any signal from an imaging experiment:

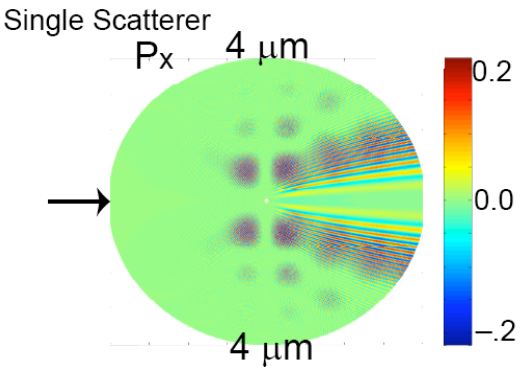

With the powerful wavepacket codes developed by Robert Parrot of our group, together with the self-consistent field modeling of Mike Stopa, we have a unique capability to model the planned and ongoing imaging experiments, namely imaging *electron flow and transconductance with and without a magnetic field*, (also in collaboration with the **Marcus** group). The backscattering in the first generation of experiments represented an ideal geometry where multiple scattering off the probe was not important, far enough away from the QPC at least. In measuring A to B conductance, the physics changes, and so will the images, but we believe our codes and theory, including soft walls, impurities, classical and quantum simulations, etc. are up to the task. A preliminary classical study of the A to B flow (in one QPC and out the other) is shown below:

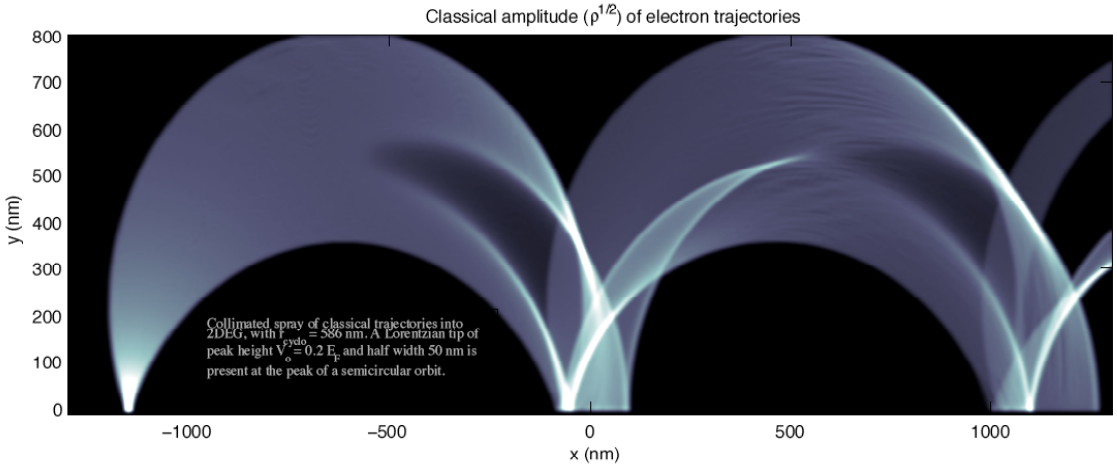

Separately, we are attempting to understand how to modify/extend the single electron thermal wavepacket code to account for *electron-electron collisions*, of the sort which lead to the correlated currents in two beams which the **Westervelt** team is attempting to measure. The single electron code we already have replaces a thermal average with a wavepacket of width equal to the thermal length; we ought to be able to run two simultaneous wavepackets (i.e., a wavepacket in four dimensions) and treat screened Coulomb scattering and somehow account for the forbidden transitions (i.e., scattering

into occupied levels). This is a fascinating problem, because the single electron thermal wavepacket code is so compelling physically, yet two electrons at the same time is fraught with conceptual and computational issues. See the single electron figure below for an idea how the thermal wavepacket accounts for backscattering interference effects which survive thermal averaging:

Charge distribution in 2DEGS

Although the nonuniform charge distribution in the delta layer has long been understood to cause low angle scattering and a limit to mobility, and more recently is known to cause the branching pattern of electron flow in 2DEGS, it has been difficult to actually access the charge distribution more or less directly. Mobilities are very indirect, branching is more direct but still hard to do the inverse scattering problem. Recently however it has become clear that opening up the QPC to many transverse modes would not wash out the electron flux fluctuation completely, but rather will leave a characteristic focal enhancement downstream of every relative positive charge cluster. This is a local effect and good data from this open mode regime should be invertible, since far upstream effects are damped out. The following image is the kind of data which might be obtained:

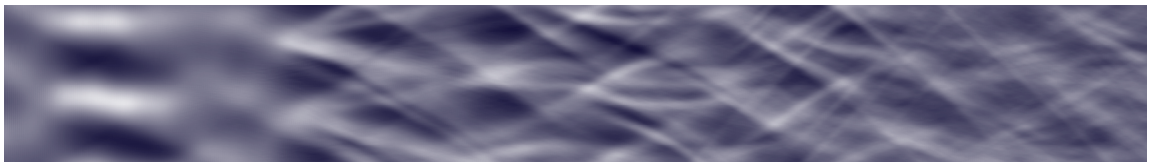

Essentially, each one of the bumps or "moguls" lies just downstream of a relatively positive charge fluctuation. Charge is flowing left to right; about 20 modes are open here.

SPM Tip Physics

It has become clear that a detailed knowledge of how SPM charged tips interact with the electron flow in the 2DEG layer is crucial not only to extracting all that can be learned from the first generation of imaging experiments, but also to moving onto the next generation. It has occurred to us that the characteristics of tip scattering, given the form of the potential, the fact that it is embedded in two dimensions, and the flux fields it finds, are all unique and point to a unique opportunity. We have formed a "working group" of all the students in my group going related work, plus Michael Stopa, **Robert Westervelt**, and some of his students. The product will be individual multi-authored papers and we hope a comprehensive review within a year or two.

Progress has been made in understanding the electrostatic effect of a charged tip, and studies are now underway as to how the tip images nontrivial (e.g., cusped) electron flow, as seen in the 2DEG data. Much insight has been gained into the very different ways the "invasive" tip probe of the transconductance measurements images electron flow compared to the self-conductance backscattering imaging.

Magnetic Force Microscope Construction for Vortex Pinning Studies

Jennifer E. Hoffman
Physics, Harvard
Collaborator: Robert M. Westervelt

The goal of this project is to detect and measure magnetic forces with 10-nm spatial resolution and sub-picoNewton force resolution. This imaging technology will be used initially for the study of superconducting vortices with a long-term interest in vortex-based computing.

Superconductors have many potential uses, including:

- macroscopic generation of large magnetic fields, for medical diagnostics or basic scientific research
- microscopic SQUIDS, for sensitive magnetic field detection in medicine, materials quality control, and many other applications

These applications are presently limited by the uncontrolled dissipative motion of vortices (magnetic flux quanta). Although much research has been devoted to understanding average vortex properties, little is known about the microscopic motion and pinning of single vortices.

On the other hand, controlled vortex motion presents new opportunities for computing. Collectively controlled vortex motion can serve as a rectifier (Villegas *et al.* 2003), a vortex ratchet mechanism can perform clocked logic (Hastings, *et al* 2003), and vortices can control spins in an adjacent diluted magnetic semiconductor (Berciu, *et al.* 2005).

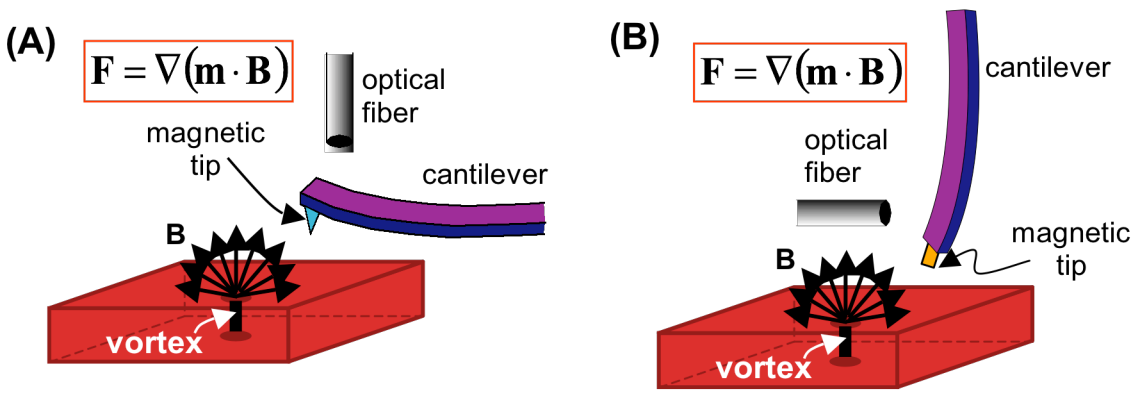

Figure 6.30. (a) Standard magnetic force microscope geometry: horizontal cantilever detects vertical force gradients. **(b)** Proposed new magnetic force microscope geometry: vertical cantilever detects horizontal force gradients. This geometry is much more suitable for studying the pinning of vortices in superconductors.

Given these challenges and opportunities, it is imperative to gain a better understanding of single vortex pinning. During the 2005–2006 fiscal year, we have been constructing a magnetic force microscope with geometry tailored to the study of vortices.

G2 student Sang Chu is currently wrapping up the MFM design. A proposed timeline is as follows:

- Fall 2005 – completed design of optical interferometer system, obtained quotes and decided on all parts (We will delay the actual purchases in order to maximize our use of the warranties on expensive parts.)
- Jan., Feb., March 2006 – MFM design nearly complete, subject to a final round of Solidworks calculations to model its mechanical properties
- end of March 2006 – submit MFM designs to Harvard machine shop
- Apr., May 2006 – fridge design (discussions already underway with Janus)
- June, July 2006 – electronics
- Aug. 2006 – begin assembly

References

J. E. Villegas *et al.*, *Science* **302**, 1188 (2003).
M. B. Hastings *et al.*, *Phys. Rev. Lett.* **90**, 247004 (2003).
M. Berciu, T. G. Rappoport, B. Jankó, *Nature* **435**, 71 (2005).

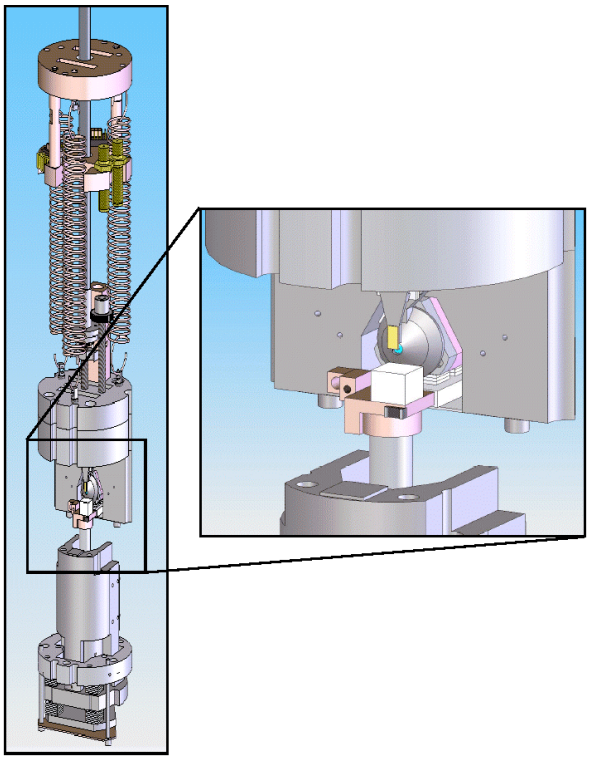

Figure 6.31. The magnetic force microscope design nears completion. The drawing shows the instrument layout, with a blow-up of the sample imaging region. The sample sits face-up on the white surface, while a magnetic-tipped cantilever (shown in yellow, just above the sample) is used to measure magnetic forces and to manipulate vortices. The magnetic force results in a deflection of the cantilever, which is measured via a laser beam reflected off the cantilever from behind (the small blue circle). The unique feature of this new imaging tool is the vertical cantilever, which allows direct detection of magnetic forces in the plane of the sample.

When complete, such a novel magnetic imaging tool may be useful not only for vortex studies, but also for imaging ever-shrinking magnetic storage bits and current patterns in nanowires.

Perhaps even more importantly, the MFM may be used not only for passive imaging, but also for active manipulation of the material or device being studied. The nanoscale magnet on the end of the cantilever may be used to drag vortices between pinning sites, to flip nanoscale bits, or to manipulate spins in diluted magnetic semiconductors.

Imaging Spins in Quantum Dots

Marc A. Kastner
Physics, Massachusetts Institute of Technology
Collaborators: Charles M. Marcus, Robert M. Westervelt (Harvard)

The long-range goal of our NSEC work is to image electron spins in quantum dots. **Westervelt**'s group has made great advances in imaging electron charge density. Imaging the spin density of electrons in nano structures will give additional information about electronic wave functions and may be useful in characterizing devices, for quantum computing for example.

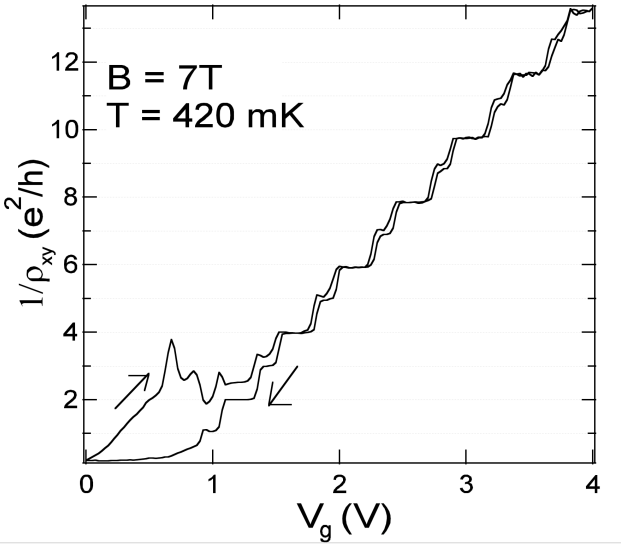

Figure 6.32. Inverse of Hall resistance as a function of gate voltage for InAs quantum well. The horizontal lines are expected values of quantum Hall resistance. Note that the spin splitting is complete for the lowest few plateaus.

The first step is to control the spin in a quantum dot. Our approach is to mount a lateral quantum dot over a hole in the wall of a microwave cavity in our dilution refrigerator. The dots have been made, so far, from GaAs heterostructures grown by the **Gossard** group. We are working with the **Marcus** group to use atomic layer deposition (ALD) of a thin oxide to gate InAs quantum wells, grown by the **Gossard** group. The very large g-value in the latter material could make spin excitations easier to control. A static magnetic field is applied parallel to the two-dimensional electron gas in the heterostructure, and the oscillating field from the cavity is oriented perpendicular to the static field. In this arrangement, microwave resonant transitions will occur between the spin states of an electron confined by nanometer-size electrodes in the quantum dot.

We have made important progress in two aspects of this project. First, we have demonstrated how to gate InAs quantum wells. This has been found to be very difficult in the past because gates relying on Schottky barriers usually leak badly. We find that the ALD oxide makes gating successful. Figure 6.32 shows the Hall conductance of an InAs quantum well as a function of gate voltage. Well-defined plateaus are observed, resulting from the quantum Hall effect. The Hall conductance is non-ideal in a variety of ways: one sees hysteresis and plateaus with lower than expected conductance. However, the successful gating promises success in making quantum dots. We are currently fabricating quantum point contacts and quantum dots in InAs using this ALD gating.

A second, very important aspect of the control of spins is the use of single-electron real-time detection. Using a commercially available voltage amplifier and a cold load resistor, we can detect the addition or subtraction of a single electron from a quantum dot. We apply a series of voltages to the quantum dot, which changes the energy of the confined electron relative to the Fermi energies in the leads. We measure the voltage across a nearby quantum point contact, to which a current is applied. Figure 6.33 shows the results of one such measurement. The measurement is done with a magnetic field B parallel to the 2DEG in the heterostructure.

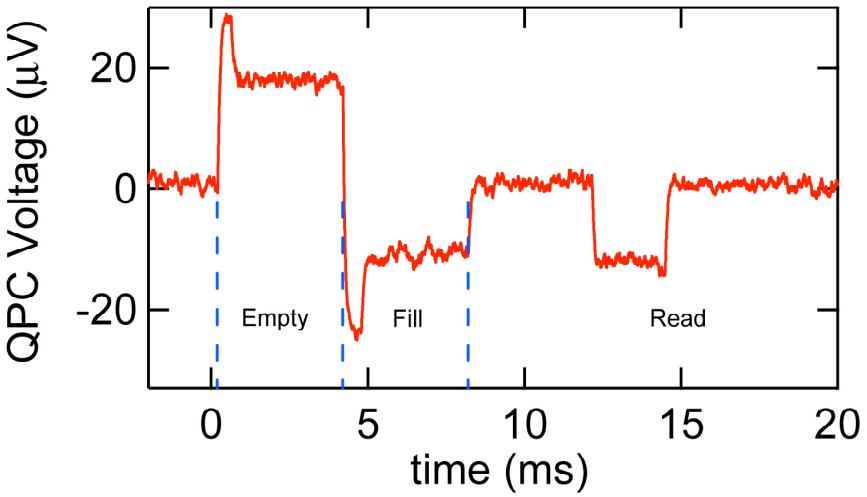

Figure 6.33. Voltage across QPC during a series of voltage steps. The first step raises the energy of the quantum dot so the dot empties of its electron. The short peak is the direct coupling of the gate to the QPC. The second step lowers the energy so the dot fills. The third step raises the energy so that the lower-energy spin state is below the Fermi energy, but the excited spin state is above the Fermi

When an electron is in the excited state, one observes a pulse as shown. By varying the fill, or waiting, time t_W, one can determine how long the electron lives in the excited state. This allows us to measure the energy relaxation rate $W = 1/T_1$. We plot W as a function of magnetic field in Figure 6.34 It agrees well with the theory of Golovich and Daniel Loss.

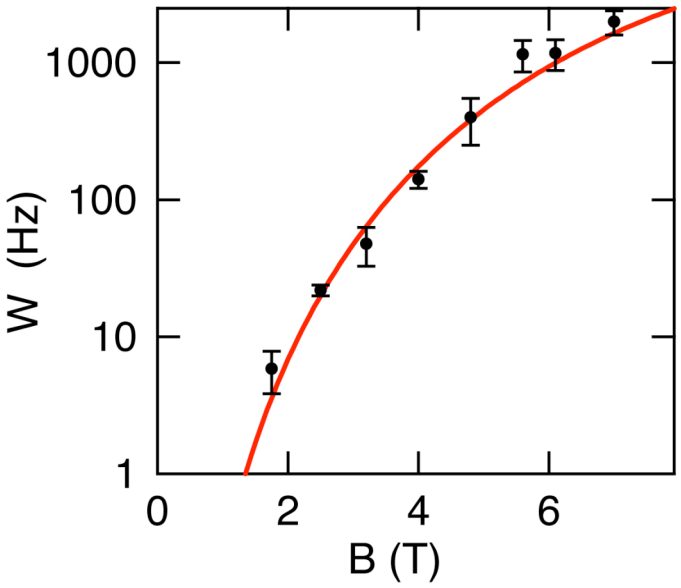

Figure 6.34. Energy relaxation rate of an electron in a quantum dot as a function of magnetic field. The red curve is the prediction of Golovach *et al.* (*Phys. Rev. Lett.* **93,** 16601, 2004).

Ballistic Electro Photonics of Nanostructures

Venkatesh Narayanamurti
Applied Physics and Physics (Harvard)
Collaborator: A.C. Gossard, P. Petroff (University of California Santa Barbara)

Over the last few years **Narayanamurti** group has pioneered the use of Ballistic Electron Emission Microscopy (BEEM) and Spectroscopy (BEES) for the study of semiconductor heterostructures below the surface. BEEM, which is a three-terminal

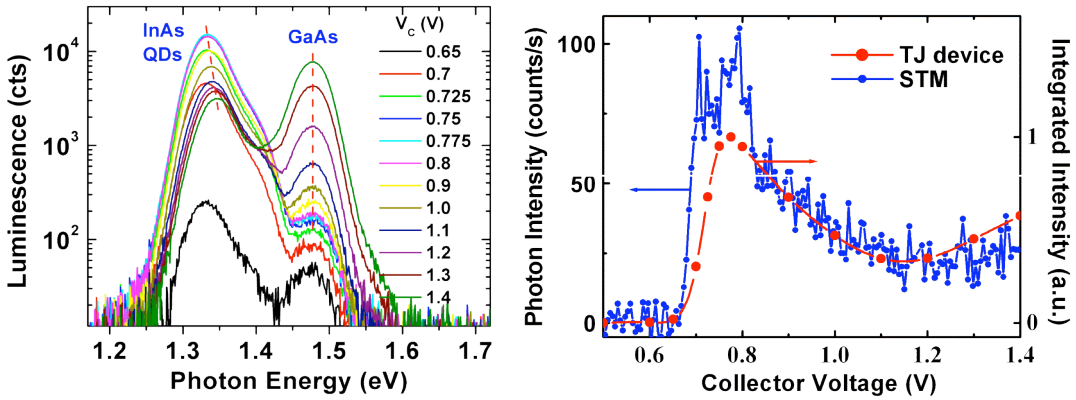

Figure 6.35. *Left:* BEEL wavelength spectroscopy of InAs quantum dots measured at 77K by solid-state tunnel-junction injection. *Right:* Spectrally-integrated spectrum from the tunnel junction device (data in left) compared to a BEEL spectrum by STM tip injection.

modification of a scanning tunneling microscope, can be used to measure the electronic band structure of a buried semiconductor heterostructure. BEEM technique provides the carrier filtration at a metal-semiconductor interface, since only the electrons that can traverse the metal base and overcome the Schottky barrier will be collected at the semiconductor substrate (collector). BEEM provides, in complement to the surface morphology, a combination of low-energy electron microscopy and spectroscopy with high spatial and energy resolution.

Currently **Narayanamurti**'s group is developing Ballistic Electron Emission Luminescence (BEEL), an extension of BEEM technique combining three-terminal

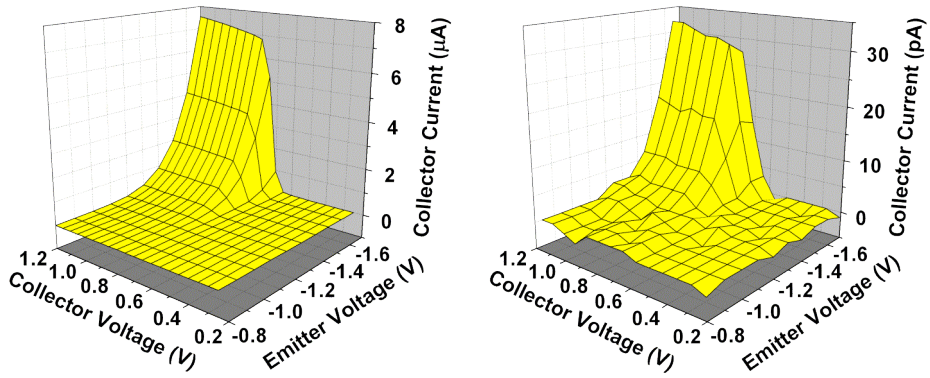

Figure 6.36. *Left*: BEES obtained from a solid-state tunnel junction device with embedded InAs quantum dots. *Right*: BEES obtained from a STM tip injection. All data were collected at or below 77K.

ballistic electron injection and interband radiative recombination in semiconductor quantum structures. BEEL provides a unique way to probe luminescent processes within semiconductors. Electrons are emitted from a tunnel junction and recombine with holes in a biased semiconductor heterostructure. The ability to vary the collector bias and the conduction-band current and simultaneously monitor the energy of emitted photons allows us to perform spectroscopy. This provides for the first time a unique capability for a comprehensive study of nano-photonic materials at a local scale. The BEEM and BEEL techniques thus allow the local determination of the band parameters, band offsets and positions of luminescent states.

The metal-base hot-electron transistor is used as a solid-state prototype for BEEL. Such a device is fabricated on the same semiconductor heterostructure, by replacing the scanning tip with a planar tunnel emitter made of aluminum and its oxide. It was utilized to perform spectrograph analysis (e.g., Figure 6.35, left) of the hot-electron induced luminescence assisted by a substantially higher current injection level. It was found to be a complementary method to analyze the luminescent states of the material studied. In the case of STM tip injection, where typical collector current is in the order of picoampere, photons emitted were collected using far-field optics and detected by an avalanche photodiode (Figure 6.35, right). Simultaneous BEES measurement was made possible by freezing out the thermionic leakage current at low temperatures (Figure 6.36). These results demonstrate the feasibility to simultaneously acquire topographic, electronic and

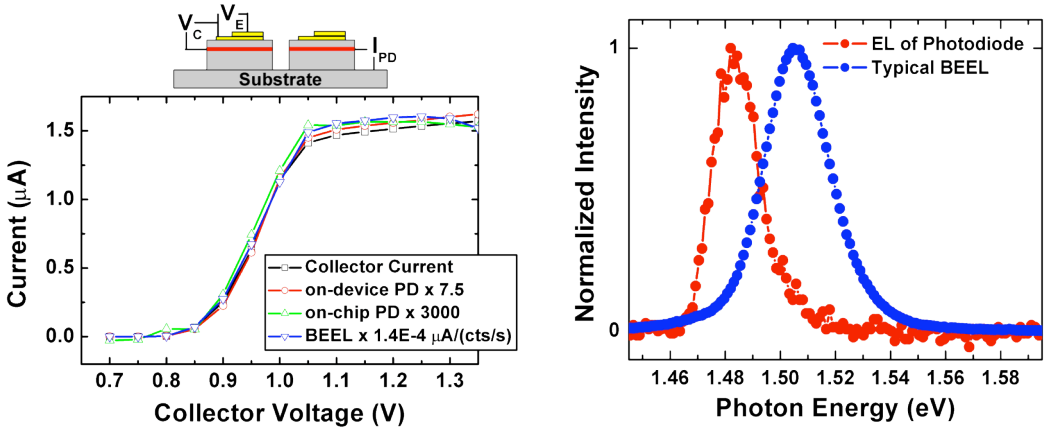

Figure 6.37 *Left:* Integrated-optics BEEL setup (above) and comparison of collector bias dependence of collector current (squares), on-device photodiode current (circles), adjacent photodiode current (up triangles) and far-field luminescence (down triangles) concurrently measured at 77 K. *Right:* BEEL spectrum and electroluminescence of forward-biased on-device photodiode at 77 K.

photonic information of buried luminescent semiconductor heterostructures.

To improve the signal-to-noise level of photon detection, the far-field optics can be replaced with an integrated *p-i-n* photo-detector, which may be monolithically incorporated into the same semiconductor substrate by epitaxial techniques. Results from solid-state hot-electron transistors fabricated using such a design could detect more than 10% of the photons emitted from the luminescent GaAs quantum well (see Figure 6.37). The improved photonic coupling and effective collection angle in this scheme improves the BEEL signal by many orders of magnitude as compared to far-field methods. Direct integration of the photo-detector into the BEEL device also eliminates the necessity for

accommodating conventional optical elements, which greatly simplified instrumentation complexity and lowered the technical entrance threshold for BEEL microscopy.

InP self-assembled quantum dots are technically important for optoelectronic applications and quantum information processing because their emission wavelength match the detectivity peak of Si photodiode. They are currently being investigated using BEEL. Dupuis group has established growth conditions for red light emitting InP quantum dots embedded in AlGaInP/GaAs system. Preliminary BEEL results on solid-state devices have demonstrated visible luminescence induced by hot-electron injection (see Figure 6.37), albeit the quantum efficiency of current devices needs to be further improved for further microscopic studies.

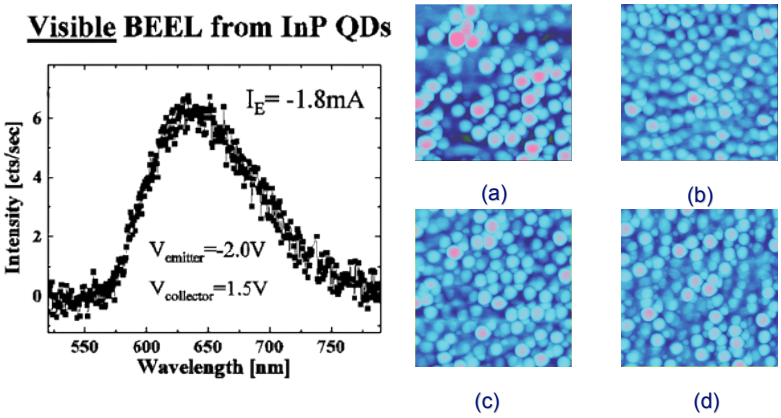

Figure 6.37. *Left:* Visible BEEL spectrum from InP quantum dots. *Right:* AFM images of InP quantum dots grown under different conditions (courtesy: R. D. Dupuis).

Understanding the Many-body Effects in Quantum Confined Structures

Pierre Petroff
Materials, University of California at Santa Barbara
Collaborators: Raymond Ashoori (Massachusetts Institute of Technology), Venkatesh Narayanamurti (Harvard)
Student and Postdoc: Mr. A. Wang (MIT), Dr. He Jun (UCSB)

This project is aimed at understanding the many-body effects associated with electrons confined in a single quantum dot. It combines an electron wave imaging technique developed in **Raymond Ashoori**'s MIT laboratory with the expertise on self-assembled quantum dot growth developed over many years at UCSB.

We have been working with **Raymond Ashoori** and his student, Mr. Albert Wang, to develop a device which will be used for imaging the wave function of single or multiple trapped electrons in a semiconductor quantum dot. The device band structure was designed in a collaborative effort with Mr. Wang who computed the band diagram of the device using a Poisson solver program. The first structure was grown at UCSB using our molecular beam epitaxy facility.

The corresponding structure shown in Figure 3.14 was grown using MBE by Dr. Jun He at UCSB. The MBE was done in such a way that a gradient in the QDs density was achieved across the wafer. This procedure should allow the imaging of a single electron wave function in a single InAs QD.

The structure was sent for characterization in **Raymond Ashoori**'s laboratory. We plan to extend this study to the imaging of electron waves in Quantum Posts (QPs). These quantum structures are essentially similar to QDs but have a height which can be adjusted through the growth process between 3 nm and 50 nm. InGaAs QPs have up to three electronic levels which are confined by their dimension along the growth direction. We believe these will provide a novel way of understanding some of the many-body effects in quantum confined structures.

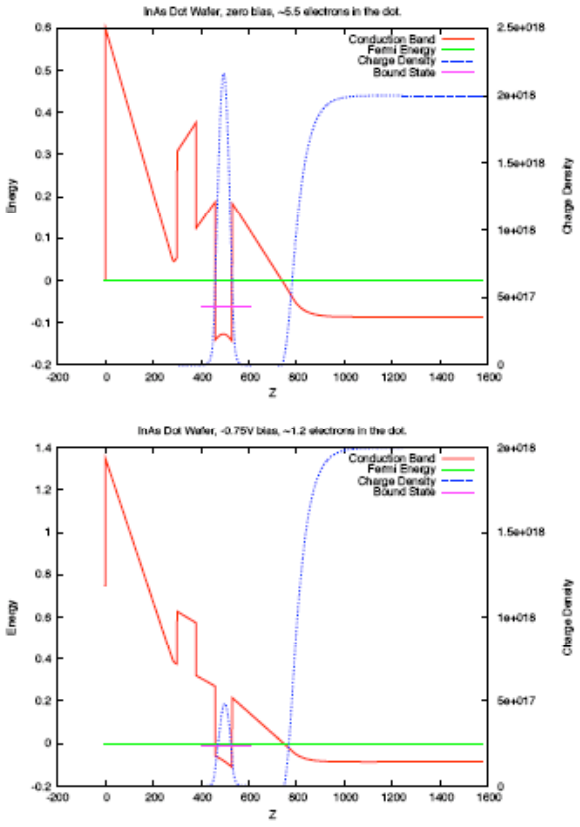

Figure 3.14. Conduction band diagram of the device structure designed for scanning probe imaging (SPI) of the electron wave function in a quantum dot. The computed charge density is shown as a dash line. The upper diagram corresponds to a voltage which allows trapping of many electrons inside the InGaAs quantum dot (QD). The lower diagram corresponds to a voltage bias producing the charging of the QD through tunneling of a single electron from the back n+ GaAs layer.

Surface

$280\,\AA$	GaAs	Undoped
$\delta-$doping	N-GaAs	2D Sheet Density $N_d = 2\times10^{12}cm^{-2}$
$20\,\AA$	GaAs	Undoped
$80\,\AA$	Al_xGa_{1-x} As	$x = 0.327$, Undoped
$80\,\AA$	GaAs	Undoped
$40-70\,\AA$	$In_xGa_{1-x}As$	$x = 0.5$, Self Assembled Dot Layer
$250\,\AA$	GaAs	Undoped
$800\,\AA$	n-GaAs	$N_d = 2\times10^{18}cm^{-3}$, Bottom Electrode

Substrate

Self Assembled Dot Density $\approx 2\times10^{9}cm^{-2}$.
Dot Lateral Size $\approx 275\AA$.

Figure 3.40. Structure of the InGaAs/GaAs/AlGaAs heterostructure sample grown by MBE for SPM imaging of the electron wave in a single QD.

Imaging Nanowires and Quantum Dots

Robert M. Westervelt
Applied Physics and Physics
NSEC Faculty Collaborator(s): Arthur C. Gossard (UCSB), Eric Heller, Michael Stopa (Harvard)
Other Outside Collaborator(s): Erik Bakkers (Philips), Leo Kouwenhoven (Delft) and Lars Samuelson (Lund)

A cooled scanning probe microscope (SPM) is a powerful tool for the investigation of the quantum behavior of electrons inside nanoscale systems. A quantum dot that contains only one electron is a leading candidate to implement a spin qubit for quantum information processing systems, as proposed by Loss and DiVincenzo. In recent research (Fallahi *et al.* 2005) we have imaged conduction through a 1-electron dot formed in a GaAs/AlGaAs heterostructure using a charged SPM tip at liquid He temperatures. When the dot is in the Coulomb blockade regime, an image of dot conduction vs. tip position shows concentric rings that correspond to Coulomb blockade peak. By adjusting the tip voltage, the size of the ring can be reduced to zero, as the last electron is pushed off the dot. These experiments show that scanning probe microscopy will be very useful for developing and testing quantum dot circuits.

Quantum dots for quantum information processing should be very small, contain one electron and have a large g-factor, so that the electron spin can be easily manipulated. Semiconductor nanowires provide very attractive building blocks. Bakkers and Kouwenhoven are developing single InAs nanowire SETs with source- and drain contacts and a back gate; they provided samples for us to image at Harvard at liquid He

temperatures. InAs is an excellent material, because it has a large g-factor, and because the electrons exist very near the surface.

Figure 6.41 shows a SPM image of conductance through one of the test devices in the Coulomb blockade regime. The conducting tip is used as a movable gate. Under the bias conditions, concentric conductance rings are observed for three quantum dots located at positions along the nanowire. The origin of the quantum dots is not clear at present. A plot of conductance vs back gate voltage show a complex pattern of Coulomb blockade peaks, and peak suppression, that are associated with dots of unequal size in series. The SPM image provides much more information: it locates the dots, and shows how the number of electrons on each dot changes with tip voltage. The image also demonstrates how one can use an SPM tip to selectively gate just one dot along the wire by moving the tip accordingly. In this collaboration we plan to study the motion of electrons through open semiconductor nanowires, and develop new nanowire devices by varying the contact materials and preparation.

The Center has begun a new collaboration with Lars Samuelson of Lund University in Sweden. By changing the semiconductor alloy as a nanowire is grown, one can create a heterostructure with a quantum dot located at a specific location. Samuelson provided devices with an InAs quantum dot with InP barriers located inside an InAs nanowire; they have source- and drain contacts and a back gate. The dot has the shape of a hockey puck, and it can be made quite small. The number of electrons can be increased incrementally from zero, and the Coulomb blockade diamonds show a characteristic shell structure in a plot of dot conductance vs. tip gate voltage and source-to-drain voltage, shown in Figure 6.42.

The InAs quantum dot in an InAs/InP nanowire can be imaged at liquid He temperatures by scanning a conducting SPM tip above, as a moveable gate. Figure 3.16 shows an SPM image of conductance vs. tip position that shows the Coulomb blockade ring separating 2 and 1 electrons on the dot. By changing the tip voltage, or the back gate voltage, the number of electrons can be reduced from 1 to 0. This example shows how SPM imaging will be a powerful tool for the manipulation of 1-electron dots in InAs/InP nanowires.

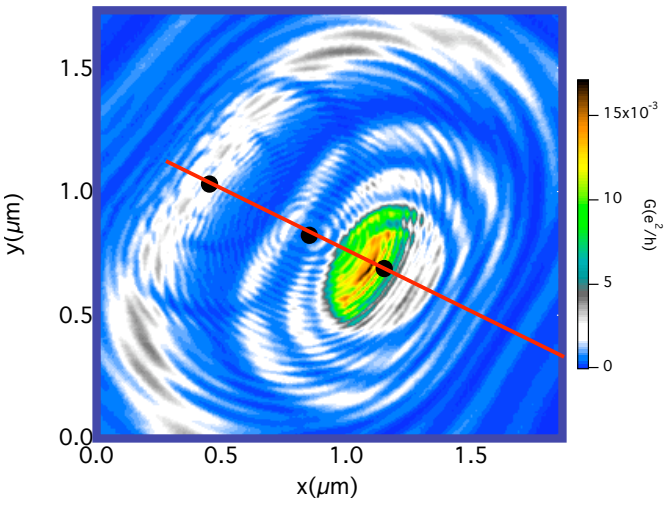

Figure 6.41. SPM image of conduction through an InAs nanowire (Bakkers and Kouwenhoven) showing nested rings from three quantum dots.

A tunnel-coupled double dot can be grown in a InAs/InP nanowire using the same growth technique. One would like to individually gate each dot to perform the kind of measurements done with lateral dots in GaAs/AlGaAs heterostructures, which have attracted a great deal of attention in recent years. However, it is difficult to individually gate each dot, because they are so closely spaced. By using a conducting SPM tip

as a movable gate, along with a back gate, we plan to investigate the interaction of two 1-electron InAs quantum dots in an InAs/InP nanowire. This approach should be a promising way to move studies of quantum information processing to higher temperatures and lower magnetic fields.

Reference

P. Fallahi, A.C. Bleszynski, R.M. Westervelt, J. Huang, J. Walls, E.J. Heller, M. P. Hanson, A.C. Gossard, "Imaging a single-electron quantum dot," *Nano Letters* **5**, 223 (2005).

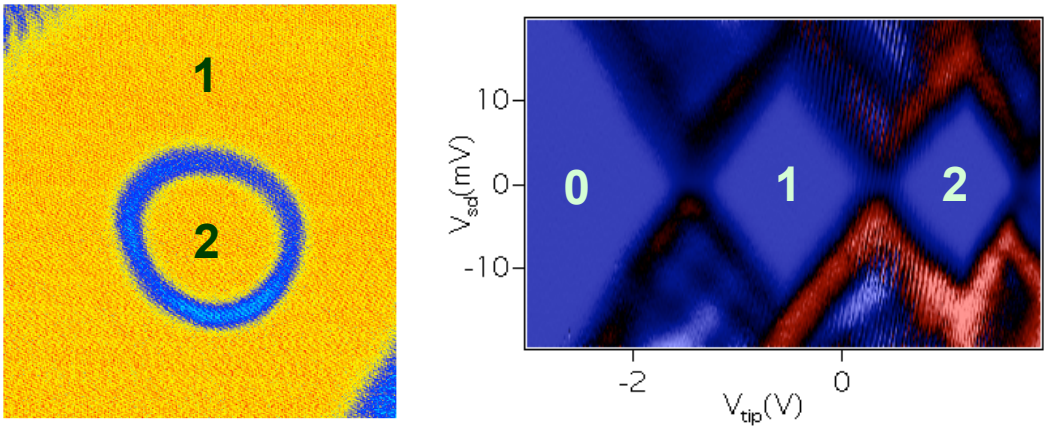

Figure 6.42. SPM image of conduction through a single quantum dot in a InAs/InP nanowire (Lars Samuelson). *(left)* SPM image showing the Coulomb blockade conductance ring between 2 and 1 electrons on the dot. *(right)* Coulomb blockade diamonds of the dot for 0, 1, and 2 electrons vs. tip voltage and source to drain voltage.